NASA TECHNICAL MEMORANDUM

NASA TM X-3007

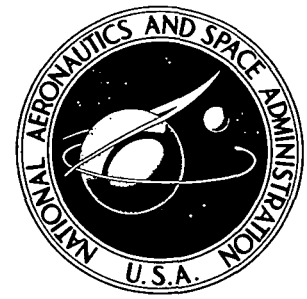

NASA TM X-3007

JET ENGINE EXHAUST EMISSIONS OF HIGH-ALTITUDE COMMERCIAL AIRCRAFT PROJECTED TO 1990

by Jack Grobman and Robert D. Ingebo

Lewis Research Center
Cleveland, Ohio 44135

NATIONAL AERONAUTICS AND SPACE ADMINISTRATION • WASHINGTON, D. C. • MARCH 1974

1. Report No.	2. Government Accession No.	3. Recipient's Catalog No.
NASA TM X-3007		

4. Title and Subtitle	5. Report Date
JET ENGINE EXHAUST EMISSIONS OF HIGH-ALTITUDE COMMERCIAL AIRCRAFT PROJECTED TO 1990	March 1974
	6. Performing Organization Code

7. Author(s)	8. Performing Organization Report No.
Jack Grobman and Robert D. Ingebo	E-7822
	10. Work Unit No. 501-24

9. Performing Organization Name and Address	11. Contract or Grant No.
Lewis Research Center National Aeronautics and Space Administration Cleveland, Ohio 44135	
	13. Type of Report and Period Covered
12. Sponsoring Agency Name and Address	Technical Memorandum
National Aeronautics and Space Administration Washington, D.C. 20546	14. Sponsoring Agency Code

15. Supplementary Notes

16. Abstract

Projected minimum levels of engine exhaust emissions that may be practicably achievable for future commercial aircraft operating at high-altitude cruise conditions are presented. The forecasts are based on (1) current knowledge of emission characteristics of combustors and augmentors; (2) the status of combustion research in emission reduction technology; and (3) predictable trends in combustion systems and operating conditions as required for projected engine designs that are candidates for advanced subsonic or supersonic commercial aircraft fueled by either JP fuel, liquefied natural gas, or hydrogen. Results are presented for cruise conditions in terms of both an emission index (g constituent/kg fuel) and an emission rate (g constituent/hr).

17. Key Words (Suggested by Author(s))	18. Distribution Statement
Jet engine exhaust emissions; Emission reduction technology; Fuel combustion; JP fuel; Liquefied natural gas fuel; Hydrogen fuel	Unclassified - unlimited Cat. 33

19. Security Classif. (of this report)	20. Security Classif. (of this page)	21. No. of Pages	22. Price*
Unclassified	Unclassified	86	$3.75

* For sale by the National Technical Information Service, Springfield, Virginia 22151

CONTENTS

JET ENGINE EXHAUST EMISSIONS OF HIGH-ALTITUDE COMMERCIAL AIRCRAFT PROJECTED TO 1990*

by Jack Grobman and Robert D. Ingebo

Lewis Research Center

SUMMARY

Forecasts of the minimum levels of exhaust emissions realistically achievable by future commercial aircraft cruising within the upper troposphere and stratosphere are presented. These forecasts are based on current knowledge of the emission characteristics of combustors and augmentors, the status of combustion research in emission reduction technology, and predictable trends in combustion systems and operating conditions as required for projected engine designs that might be used by future subsonic and supersonic commercial aircraft fueled by either JP fuel, liquid natural gas, or hydrogen. Results are presented for cruise conditions in terms of both an emission index (g constituent/kg fuel) and an emission rate (g constituent/hr).

INTRODUCTION

This report forecasts the minimum realistic levels of exhaust emissions for future commercial aircraft operating at high-altitude cruise conditions. Such predictions are needed by the Department of Transportation as input to the Climatic Impact Assessment Program (CIAP). The purpose of CIAP is to assess, by 1974, the potential climatic effects of perturbations of the upper atmosphere caused by the propulsion effluents of a world-wide high-altitude aircraft fleet to the year 1990 and beyond (ref. 1, pp. 2-12). One of the principal efforts of the overall program is the preparation of six monographs on (1) the natural stratosphere of 1974, (2) the nature of propulsion effluents, (3) the perturbed stratosphere, (4) the perturbed troposphere, (5) biological effects, and (6) economic effects. The engine emission forecasts provided herein will be used as

---

* The information presented herein is included in chapter 5 of volume II, "Nature of Propulsion Effluents," as part of the Climatic Impact Assessment Program sponsored by the Department of Transportation.

part of the input to the second monograph and will be combined with projections of future aircraft routes and frequency of travel to determine the rate of introduction of engine effluents into the stratosphere from advanced subsonic and supersonic commercial aircraft.

Current pollution technology investigations at the NASA Lewis Research Center, both small-scale and full-annular combustor test efforts, are aimed at initiating and evaluating potentially attractive techniques for reducing exhaust emissions from jet aircraft. These efforts will provide an estimate of the extent to which current and future combustor emission levels can be reduced. Some techniques being evaluated are air atomizing, premixing, and prevaporizing fuel-injection systems; multizone fuel distribution; fuel staging, variable geometry for airflow, and/or fuel distribution control; exhaust gas recirculation; reduced reaction-zone dwell time; rapid reaction-zone mixing; and the use of alternate fuels. In addition, information from engine cycle studies is being used to forecast the operating constraints that may be imposed on the combustor. These techniques and results are combined to make a NASA forecast of practicably achievable low-emission engine technology for the time periods of 1980-85 and 1990 and beyond. These forecasts are made on the premise that conventional JP fuel will continue to be the only aircraft fuel that is used until the late 1990's. The use of conventional JP fuel, liquefied natural gas (LNG), and hydrogen is considered for the time period beyond the late 1990's.

Exhaust emissions predicted for projected propulsion systems for future commercial jet aircraft are presented for both minor and major redesigns of the combustor which implement low-emission technology. In addition, theoretical minimum emission limits were determined from chemical kinetics calculations for a combustor using premixed-prevaporized fuel. The emission forecasts are presented for cruise conditions in terms of both an emission index (g constituent/kg fuel) and an emission rate (g constituent/hr). Emission forecasts include estimates for oxides of nitrogen, carbon monoxide, total hydrocarbons, particulates (soot), sulfur dioxide, and trace elements, in addition to carbon dioxide and water.

EMISSION CHARACTERISTICS OF GAS TURBINE COMBUSTORS AND AUGMENTORS

We shall briefly review the emission characteristics of jet engines, particularly during high-altitude cruising. Many reports (refs. 2 to 4) discuss the relative contribution of jet aircraft emissions from ground and low-altitude maneuvers to urban pollution. Even though the overall contribution of aircraft to urban pollution is small, the air quality in the vicinity of commercial airports is considered to be significantly affected by jet aircraft emissions. During idling and taxiing, the principal pollutants are un-

burned hydrocarbons and carbon monoxide; during landing and takeoff, they are oxides of nitrogen and smoke. Emission data for a number of commercial jet engines for subsonic aircraft are documented in reference 5. These data apply mainly to operating modes below an altitude of 900 meters, which include idle, takeoff, climbout, descent, and landing. These data were obtained by ground-based sampling of the exhaust from jet engines operating at sea-level conditions over a range of engine speeds that simulated the various operating modes.

Data on the emissions of supersonic aircraft at cruise conditions are presented in reference 1. The constituents of the engine exhaust are mainly a function of the combustor operating conditions, including combustor inlet total temperature and pressure, combustor reference velocity or reaction dwell time, and fuel-air ratio. Cruise emissions from either subsonic or supersonic jet aircraft may be predicted from their combustor operating conditions during cruise by using typical emission data correlations obtained over a range of combustor operating conditions.

During cruise, the products of incomplete combustion (carbon monoxide and hydrocarbons) are relatively low in concentration, because gas turbine combustors operate at a combustion efficiency near 100 percent at cruise conditions. The concentrations of carbon monoxide and hydrocarbons would be slightly higher in the exhaust of an afterburning turbine engine than in that of an unaugmented engine, since afterburners tend to burn less efficiently than main combustors.

Nitric oxide is considered to be the most significant emission product formed during altitude cruise. The quantity of nitric oxide formed in the combustor is a strong function of flame temperature, which increases with increasing combustor inlet total temperature. Combustor inlet total temperature increases with increases in either compressor pressure ratio or flight Mach number.

Constituents in Jet Engine Exhaust

The various constituents in a jet engine exhaust under typical takeoff and cruise conditions are given in table I. The constituents have been grouped by source into five categories: (1) inert substances and unreacted oxygen from air, (2) products of complete combustion of fuel, (3) products of incomplete combustion, (4) oxides of nitrogen formed during the heating of air, and (5) elements or compounds derived from sulfur and trace metals present in kerosene fuel. The concentrations of the components in the air and the products of complete combustion were determined for an overall fuel-air ratio of 0.014 and commercial Jet A-1 kerosene fuel. This fuel-air ratio generally ranges from 0.01 to 0.03 during cruise. The products of incomplete combustion include carbon monoxide, unburned fuel, partially oxidized hydrocarbons (such as aldehydes), hydrogen,

and particulates (soot) that consist mainly of carbon. Combustors for gas turbine engines are designed to operate with maximum performance during cruise; the estimated concentrations of the products of incomplete combustion shown in table I are equivalent to an overall combustion inefficiency of about 1 percent or less. Afterburners for gas turbine engines tend to be less efficient than the main combustors, so the concentrations of the products of incomplete combustion are generally several times greater for such augmented engines.

Oxides of nitrogen are formed from the reactions of oxygen and nitrogen at the elevated temperatures in the reaction zone of the combustor. These oxides of nitrogen (NO_x) generally consist of 90 to 95 percent nitric oxide (NO); the remainder is nitrogen dioxide (NO_2). The quantity of nitric oxide formed is affected by a number of factors, including engine compressor pressure ratio, flight Mach number, fuel-air ratio, and combustor design.

Commercial specifications for Jet A-1 kerosene require that the sulfur concentration in the fuel not exceed a value of 0.3 percent by weight. In practice, the sulfur concentration is generally less than 25 percent of this value. The sulfur in the fuel is mostly converted into sulfur dioxide (SO_2), with lesser amounts of sulfur trioxide (SO_3). Such trace metals as aluminum, iron, manganese, nickel, sodium, potassium, and vanadium are present in the fuel. The total concentration of the trace metals in jet engine exhaust is estimated to be about 5 to 20 parts per billion.

Typical Jet Engine Emission Characteristics

Figure 1 illustrates the carbon monoxide (CO), total hydrocarbon, and NO_x emissions over a range of engine speeds for a typical subsonic-aircraft gas-turbine engine with a compressor pressure ratio of 13.4 using JP-5 fuel (similar to Jet A-1). The term "emission index" (grams of constituent per kilogram of fuel burned) is used instead of the more familiar volumetric concentration term (parts per million) to normalize emissions on the basis of fuel flow. The emission index may be calculated from the volumetric exhaust concentrations for any constituent x by the following expression:

$$EI_x = 10^{-3}\left(\frac{M_x}{M_e}\right)\left(\frac{1+f}{f}\right)(x)$$

where

EI_x emission index, g of x/kg of fuel burned

M_x molecular weight of x

M_e average molecular weight of exhaust gases

f fuel-air ratio

x concentration of x, ppm by volume

At a fuel-air ratio of 0.015, an emission index of unity is equivalent to either 15 ppm CO, 30 ppm C total hydrocarbons, or 10 ppm NO_x. The NO_x emission index is calculated by expressing all oxides of nitrogen as NO_2. At low engine speeds, corresponding to idle operation, the CO and total hydrocarbon emissions are at their highest; whereas NO_x emissions are at their lowest. At an engine speed of 100 percent, corresponding to takeoff conditions, the NO_x emissions are highest; whereas CO and total hydrocarbon emissions approach their minimum. For a subsonic aircraft, CO and total hydrocarbon emission levels at cruise would be expected to be similar to the levels during takeoff, but NO_x emissions would be lower than at takeoff.

Table II gives the main emission products, together with their major causes. A range of emissions at idle, takeoff, and cruise is shown for typical subsonic commercial engines. High total hydrocarbon and CO emissions that occur only during idle are caused by inefficient combustion. Inefficient combustion results from a combination of poor fuel atomization at low fuel-flow rates, lean reaction-zone fuel-air ratios, and low combustor inlet pressures and temperatures. Higher NO_x emissions during takeoff or cruise are caused by the increased oxygen-nitrogen reaction rates at higher flame temperatures, which result from high combustor inlet temperatures. Smoke density is high at takeoff because of high combustor pressures and rich reaction-zone fuel-air ratios. Only nitric oxide is formed in any significant quantities during subsonic cruise, but the NO_x emission index during cruise is less than that during takeoff because the combustor inlet temperature and pressure are lower.

Comparison of Subsonic and Supersonic Engines

Figure 2 shows a typical turbofan engine used on subsonic aircraft. The main engine components include a fan, a compressor, a combustor, and a turbine. A portion of the air passing through the fan enters the compressor; the remaining air is bypassed around the core engine to provide additional thrust. The flow rate and the total temperature and pressure of the air entering the combustor from the compressor discharge are established by the overall fan and compressor pressure ratio, the flight altitude, and the flight speed. The fuel-air ratio is determined by the combustor temperature rise required to obtain the design turbine inlet temperature. The frontal area of the combustor generally does not exceed the required frontal area of the compressor or turbine, in order to avoid unnecessary engine drag. The overall length of the combustor is kept as

short as practical to minimize engine shaft length and bearing requirements. The combustor shown in the drawing is of the can-annular type, in which a number of tubular combustion liners are arranged within a common annular housing. Most recent engines use an annular combustor, with a continuous combustion liner installed within an annular housing.

A schematic drawing of a conventional annular combustor is shown in figure 3. The combustor consists of three main parts: a diffuser, the primary (reaction) zone, and the secondary (dilution) zone. The diffuser is used to slow the relatively high-velocity airflow discharging from the compressor in order to produce a high static pressure. Lower combustor velocities are necessary to obtain stable combustion and to avoid excessive combustor pressure loss. Fuel is generally injected by pressure-atomizing nozzles, and combustion is initiated and stabilized in the primary zone. Enough air is introduced into the primary zone through swirlers around the fuel nozzles or through openings in the liner wall to maintain a nearly stoichiometric mixture of fuel and air. Air bypassing the primary zone is injected into the secondary zone through additional openings in the liner and is mixed with the hot gases from the primary zone to achieve the desired turbine inlet temperature distribution. The remaining airflow is used to film cool the walls of the chamber. Most of the chemical reactions are completed prior to dilution in the secondary zone. Consequently, the chemistry of the emission products is essentially frozen near the exit of the combustor.

Figure 4 is a drawing of one type of engine suitable for powering a supersonic aircraft. The main differences between the afterburning turbojet shown in this figure and the turbofan engine shown in figure 2 are (1) incorporation of an inlet diffuser (not shown) to slow the air to subsonic speeds before it enters the engine; (2) omission of a fan and bypass duct; (3) addition of an afterburner to provide thrust augmentation; and (4) installation of a supersonic exhaust nozzle. Afterburning turbojet engines similar to that shown in figure 4 are used on the Concorde SST and were intended to be used on the Boeing SST.

The afterburner consists of an inlet diffuser to slow down the turbine discharge gases, an array of fuel-spray bars followed by an array of flameholders, and a combustion chamber that is air cooled and acoustically damped to prevent screech. From a combustion point of view, the operating conditions in an afterburner are generally more severe than in the main combustor; and, therefore, the afterburner combustion efficiency tends to be lower.

Recent analytical studies (ref. 6) show that an augmented turbofan, such as the duct-burning turbofan depicted schematically in figure 5, may be an attractive choice as an engine for an advanced supersonic transport because it offers reduced jet noise during takeoff and landing. Thrust augmentation in the duct-burning turbofan is obtained by burning additional fuel in the fan discharge air duct. A variable-area exhaust nozzle is

required on both the core and bypass duct. The experimental performance of a full-scale duct burner designed for a supersonic duct-burning turbofan engine is described in reference 7.

The cruise operating conditions of representative subsonic turbofan, supersonic afterburning turbojet, and supersonic duct-burning turbofan engines are compared in the section PROJECTED ENGINE CYCLES. An efficiency of nearly 100 percent is achieved in the main combustor during cruise for all these engines, so minimum quantities of total hydrocarbons and CO are formed. The afterburner and duct-burner combustion efficiencies would be expected to be several percent less than that of the main combustor. The main factor affecting the formation of nitric oxide in either type of engine is the combustor inlet total temperature. Increasing either the compressor pressure ratio or the flight speed results in an increase in combustor inlet total temperature. Data taken for several engines at various simulated altitude conditions (refs. 8 to 11) indicate that afterburning does not significantly alter the overall NO_x emission index for supersonic aircraft.

Effect of Operating Variables on Emissions

Combustor emissions. - Total hydrocarbon, carbon monoxide, and oxides-of-nitrogen concentrations are determined mainly by combustor operating conditions.

Total hydrocarbons and carbon monoxide: Combustion efficiency can be defined as the ratio of the actual enthalpy rise to the theoretical enthalpy rise attainable for the amount of fuel used. The theoretical enthalpy rise assumes that the combustion reaction proceeds to completion to form gaseous products of combustion in equilibrium at the combustor exit temperature. Previous studies (e.g., ref. 12) have correlated combustion efficiency against a combustion parameter composed of inlet total pressure P_3, multiplied by inlet total temperature T_3, and divided by reference velocity V_r, where reference velocity is equal to the combustor airflow rate divided by the product of the air density at the combustor inlet and the maximum cross-sectional flow area of the combustor. The numerical subscripts used herein refer to axial locations along the engine's flow path as indicated by the engine stations shown in figures 2, 4, and 5.

A combustion efficiency correlation for a ram-induction combustor (ref. 13) plotted in figure 6 shows that combustion efficiency increases as combustor inlet pressure and temperature increase and decreases as combustor velocity increases. Typical values of the correlation parameter for takeoff and cruise fall far to the right of the bend in the curve, so there are no significant problems in obtaining good combustion efficiency for these conditions. At engine idle, the value of the correlation parameter is low; for this condition, obtaining good combustion efficiency is difficult. As expected, the emission

indices for CO and total hydrocarbons decrease with increasing values of the correlation parameter. Plots of the CO and total hydrocarbon emission indices against the correlation parameter are shown in figure 7. Ranges of the correlation parameter are shown for typical engines operating at idle, takeoff, and cruise conditions.

The variation in total hydrocarbon and CO emissions with combustion efficiency is shown in figure 8 (ref. 14). The curves shown in this figure represent an average variation of a band of results and are used only to illustrate the trends and are not necessarily absolute values. Significant decreases in the emission index of these pollutants are indicated with increasing combustion efficiency. For example, improving efficiency from 94 percent to nearly 97 percent (typical high-pressure-ratio engine idle efficiency) would indicate reductions of approximately 30 and 75 percent, respectively, in emissions of total hydrocarbons and carbon monoxide. Further increases in efficiency to 99 percent or higher at idle operating conditions may be possible with advanced combustor designs, indicating that further reductions in these two pollutants are possible.

Oxides of nitrogen: Figure 9 shows the effect of engine pressure ratio on NO_x emissions at takeoff (ref. 15). The increase in the NO_x emission index with increasing engine pressure ratio is caused principally by higher combustor inlet total temperatures. Higher flame temperatures, which result from combustor inlet total temperatures becoming higher as engine pressure ratio increases, produce higher emission levels for the oxides of nitrogen. Emissions of NO_x tend to increase exponentially with increasing flame temperature. This effect is illustrated in figure 10 for a variety of current production engines (ref. 14). The curve represents a nominal characteristic drawn through data points of many engines operating at takeoff conditions. It does not represent one engine operating at a varying pressure ratio. For comparative purposes, the upper limit of the curve represents an engine with a 25:1 pressure ratio; an engine with a pressure ratio of 13:1 would correspond to an inlet temperature of approximately 600 K. For a given subsonic engine, the combustor inlet total temperature and pressure during cruise are less than at takeoff because the ambient temperature and pressure are lower at the cruise altitude and because corrected engine speed is lower; therefore, NO_x emissions at cruise are less than at takeoff. For a supersonic aircraft, the combustor inlet total temperature increases significantly with increases in flight Mach number, and thus can result in increases in NO_x emissions.

Oxides-of-nitrogen emission indices have been correlated with operating variables for three swirl-can combustor models; as shown in figure 11 (ref. 16). These variables include combustor inlet total pressure and temperature, combustor exit average temperature, reference velocity, and a flame-stabilizer wetted-perimeter WP term that is related to the degree of mixing in the reaction zone. The rate of formation of NO_x is

shown to increase exponentially with inlet temperature, to increase linearly with either exit temperature or the reciprocal of reference velocity (dwell time), and to increase with the square root of pressure. The correlation presented in reference 16 represents a preliminary attempt to define the effects of a number of operating variables for a given type of experimental combustor, as evaluated over a limited range of test conditions which may not be applicable to all combustor types. Increasing combustor inlet temperature increases the flame temperature and hence the rate of formation of NO_x. Increasing combustor inlet pressure also tends to increase the formation of NO_x, but its effect is less significant. The effect of pressure might be attributed to both chemical kinetics and fuel-air mixing. Increasing combustor reference velocity tends to reduce reaction-zone dwell time, thus reducing the quanitiy of NO_x formed since the formation of NO_x is reaction-rate limited.

In general, increasing the overall fuel-air ratio has been observed to increase NO_x formation. Theoretically, the local fuel-air ratio in the primary (reaction) zone should have a very significant effect on NO_x formation by its effect on flame temperature. Flame temperature should be near a maximum at stoichiometric conditions and should be lower for fuel-air mixtures that are either leaner or richer than stoichiometric. Gas turbine combustors are generally designed so that the primary-zone fuel-air ratio is near stoichiometric in order to optimize combustion performance. Operating with a primary zone that is fuel lean leads to unstable combustion, while operating on the fuel-rich side causes excessive carbon formation. Even if the reaction zone were operated either leaner or richer than stoichiometric, factors that affect the homogeneity of the reactants, such as the fuel-air mixing intensity, fuel droplet size distribution, and fuel evaporation rate, are as important to NO_x formation as the average local fuel-air ratio in the reaction zone.

Augmentor emissions. - As in the case of the combustor, operating conditions primarily determine the emissions in augmentors.

Total hydrocarbons and carbon monoxide: Afterburners for military aircraft tend to operate at relatively low combustion efficiencies, typically of the order of 89 percent, because of the difficulty of rapidly mixing and burning fuel at relatively high velocity. At such a low combustion efficiency, total hydrocarbons and CO emission indices are quite high, of the order of 50 and 220, respectively, as shown in figure 8. However, afterburners or duct burners designed for future commercial supersonic aircraft would be required to operate with at least 98 percent combustion efficiency during cruise. In this case, total hydrocarbons and CO emission indices would be approximately 10 and 60, respectively.

Oxides of nitrogen: Tests of afterburning engines in altitude chambers (refs. 8 to 11) indicate that the fuel burned in the afterburner does not significantly alter the NO_x emission index measured at the combustor exit. The emission index for NO_x formed in

the duct burner of an augmented turbofan would be expected to be low because of the relatively low duct-burner inlet temperature.

STATUS OF EMISSION REDUCTION TECHNOLOGY OF COMBUSTORS AND AUGMENTORS

Combustor operating variables, such as combustor inlet total pressure and temperature and overall fuel-air ratio, are determined by the design of the propulsion system and the flight envelope of the aircraft. Factors affecting engine design are discussed in reference 6. A discussion on advanced engine selection is included in this report in the section PROJECTED ENGINE CYCLES. Combustor reference velocity must be limited to prevent excessive pressure losses. Thus, the only means readily available to the combustor designer to control emissions are the method of fuel atomization, the mixing of fuel and air, and the general geometry of the combustor. Of course, the selection of a fuel with chemical and/or physical properties that are significantly different from conventional kerosene (JP fuel) may also have an important effect on exhaust emissions. Preliminary research on the subject of emission reductions in gas turbine combustors is discussed in references 13 to 31.

This section summarizes some of the NASA Lewis Research Center's recent efforts in reducing exhaust emissions from turbine engines. Various techniques employed and the results of testing are briefly described and referenced for detail. The effort arises from the increasing concern for the measurement and control of emissions from gas turbine engines. The greater part of this research is focused on reducing the oxides of nitrogen formed during takeoff and cruise in both advanced conventional-takeoff-and-landing (CTOL), high-pressure-ratio engines and advanced supersonic aircraft engines. The experimental approaches taken to reduce NO_x emissions include the use of multizone combustors incorporating reduced dwell time, fuel-air premixing, air atomization, fuel prevaporization, and gaseous fuels. In the experiments conducted to date, some of these techniques have been more successful than others in reducing NO_x emissions. In all cases, considerably more research will be required to develop combustors that employ one or more of these experimental techniques without sacrificing overall combustor performance. Tests are being conducted on full-annular combustors at combustor inlet total pressures to 6 atmospheres and on combustor segments at pressures to 30 atmospheres.

As stated previously, emissions of unburned hydrocarbons and CO are caused by poor combustion efficiency at conditions such as engine idle. The use of fuel staging in multizone combustors and air-assist fuel nozzles has indicated that large reductions in hydrocarbon and CO emissions can be achieved. Studies are also being conducted on the

use of diffuser bleed and variable combustor geometry to try to optimize the combustor airflow distribution over the wide range of operating conditions. The emission characteristics were determined for Jet-A kerosene, natural gas, propane, and hydrogen fuels.

Combustor Test Procedures

Combustor testing is conducted in a variety of connected-duct test facilities at the Lewis Research Center. All inlet-air temperatures are obtained without vitiating the inlet airflow. Several test facilities have vitiating heaters to raise the inlet temperature still higher; however, they are never used during tests where the measurement of combustor pollutant levels is required. For full-annular combustors, tests can be conducted at exact conditions simulating high-altitude, high-Mach-number flight. Each test facility is equipped with on-line gas analysis instruments for pollutant measurements. The exhaust constituents, CO_2 and CO, are measured by using nondispersive infrared (NDIR) instruments; the oxides of nitrogen, NO and NO_2, are measured by using chemiluminescence instruments equipped with a thermal converter to reduce NO_2 to NO prior to measurement. Unburned hydrocarbons are measured by using a flame-ionization detector maintained at a temperature of 450 K. Unburned hydrocarbons from kerosene fuels are assumed to have the composition CH_2.

Gas sampling techniques vary from test to test. Most samples are taken from one or more internally manifolded fixed rakes. Some gas samples are taken with traversing probes in both segment and annular combustor tests. The samples are transported to the gas analysis instruments through heated stainless-steel tubes. Sample transit time through the transfer tube is minimized by venting a large amount of the sample flow at the instruments and by maintaining the pressure in the transfer tube at approximately 2 atmospheres. The sampling procedures and techniques used follow the guidelines specified in SAE ARP 1256 (ref. 32). Smoke measurements are also made by sampling at the combustor exhaust plane. The smoke number is determined by collecting the particulates on filter paper and obtaining a reflectance reading of the stain. This technique has been standardized in SAE ARP 1179 (ref. 33).

The representativeness of the gas sample is checked by comparing the computed gas-sample fuel-air ratio to the fuel-air ratio calculated from flow-rate measurements. Only data obtained where these fuel-air ratios agree within ±15 percent are accepted.

Combustor Design Philosophy

Oxides of nitrogen. - The two principal methods for reducing nitric oxide emissions are reducing the reaction-zone temperature (flame temperature) and reducing the

reaction-zone dwell time. The reaction-zone temperature may be reduced by (1) operating with either a fuel-rich or fuel-lean reaction zone, (2) operating with a more homogeneous fuel-air mixture, or (3) introducing inert substances into the reaction zone. The reaction-zone fuel-air ratio may be shifted by altering the combustor airflow distribution. However, rich reaction zones tend to form excessive amounts of CO, total hydrocarbons, and smoke, while lean reaction zones present severe combustion stability problems. If this approach is used, variable geometry might be required to continuously control combustor airflow distribution in order to avoid poor combustion efficiency and to minimize the emission products from incomplete combustion.

The fuel-air mixture could be made more homogeneous either by increasing mixing intensity, by premixing the fuel and air before they enter the reaction zone, by prevaporizing the fuel before it enters the reaction zone, or by increasing the number of fuel-injection points. Inert substances that might be used to reduce flame temperature include water or recirculated combustion products. Water injection would be impractical during cruise because of payload penalties. A significant increase in the amount of combustion products recirculated in the reaction zone might require excessive pressure losses. The reaction-zone dwell time could be reduced either by shortening the length of the reaction zone or by increasing the number of local burning zones in order to reduce the recirculation path length.

Carbon monoxide and total hydrocarbons. - Gas turbine combustors operate very near 100 percent combustion efficiency during both takeoff and cruise, and concentrations of carbon monoxide and hydrocarbons are quite low. Thus, no specific effort is being devoted to seeking further reductions at these operating conditions. Nevertheless, considerable effort is being devoted to the reduction of CO and hydrocarbons at the idle operating condition, as reported in reference 13.

Research Concepts

Multizone combustors. - Multizone combustors have shown considerable promise in reducing NO_x emissions.

Combustor descriptions: Full-annular combustor testing at Lewis has emphasized two multizone combustor concepts for decreasing burning-zone length. These are the swirl-can combustor and the double-annular combustor. The swirl-can combustor is shown in figures 12 and 13. The combustor is of annular design, 0.514 meter long and 1.067 meters in diameter. The combustor consists of 120 individual swirl-can modules which distribute combustion uniformly across the annulus. The modules are arranged in three concentric rows with fuel flow independently controlled to each row. There are 48 modules in the outer row, 40 in the center, and 32 in the inner row. The combustor

module design is shown in figure 14. Each module premixes fuel with air in the carburetor, swirls the mixture, stabilizes combustion in its wake, and provides interfacial mixing areas between the bypass air through the array and the hot gases in the wake of the module. More detailed information on swirl-can combustors can be found in references 23 to 25.

The other full-annulus combustor being investigated with a shortened burning zone is referred to as a double-annular, ram-induction combustor. A cross-sectional sketch of this combustor is shown in figure 15. Constructing the combustion zone as a double annulus permits the reduction of overall combustor length while maintaining an adequate ratio of length to annulus height in each combustion zone. This feature allows a considerable reduction in length to be made over a single annulus with the same overall height. Individual control of the inner- and outer-annulus fuel systems of the double-annular combustion zone provides a useful method for adjusting the outlet radial temperature profile. The ram-induction combustor differs from the more conventional combustors in that the compressor discharge air is allowed to penetrate into the combustion and mixing zones without diffusing to as high a static pressure. The kinetic energy of the inlet air is thereby used to promote rapid mixing of air and fuel in the primary zone and of diluent air and burned gases in the secondary zone. The airflow is efficiently turned into the combustor by two rows of vaned turning scoops that penetrate into the combustor. A more detailed discussion of the ram-induction concept is provided in references 34 to 38.

Oxides-of-nitrogen emissions: The NO_x emissions for the multizone combustors are shown in figure 16. Also shown in this figure are data from a single-annular combustor (refs. 39 and 40). The NO_x emission index (grams of NO_2 produced per kilogram of fuel burned) is shown as a function of the combustor exit average temperature. The test conditions (combustor inlet total pressure and temperature and reference velocity) were the same for all three combustors. The number of fuel-injection sources of each combustor is indicated on the curves. Increasing the number of fuel-injection sources and spreading the combustion more uniformly throughout the combustor appears to be a very effective way of reducing the emission of NO_x. The techniques of premixing fuel and air and rapid quenching of the combustion reaction, both incorporated into the swirl-can approach, are also considered to be principal factors in producing the lower NO_x emissions of these combustors. Figure 17 compares the NO_x emission level for the three combustor types with increasing inlet total temperature and a constant exit average temperature of 1500 K. The trend with increasing inlet total temperature is an exponential increase in NO_x emission index. At an inlet total temperature of 750 K, the swirl-can combustor produces only 60 percent as much NO_x as the more conventional single-annular combustor. Figure 18 shows the emissions of NO_x for the swirl-can combustor for inlet total temperatures to 840 K and fuel-air ratios to 0.0695. For the

Jet A fuel used in these tests, the stoichiometric fuel-air ratio is 0.0676. This swirl-can combustor was designed for near-stoichiometric operation and as such is larger than would be required for operation at more usual turbine inlet temperatures. The figure shows a strong dependence of NO_x emissions on both inlet total temperature and fuel-air ratio. However, as the fuel-air ratio is increased, the formation of NO_x eventually reaches a constant level; and as stoichiometric fuel-air ratios are approached, the measured concentrations of NO_x decline. Though this effect is only clearly demonstrated at an inlet total temperature of 590 K, there is no reason to believe that similar effects would not be observed at the higher combustor inlet total temperatures. A more complete discussion of all the emission characteristics of swirl-can combustors is given in references 13 and 23.

The effect of combustor residence time on NO_x emissions is shown in figure 19 for the two multizone combustors. Increasing the combustor reference velocity (decreasing the residence time) causes a corresponding decrease in the NO_x emission level. The effect is virtually linear with residence time, as is indicated by the dashed line with a slope of -1.

Smoke number: The smoke emissions of the swirl-can combustor are shown in figure 20. These data were obtained during a test to stoichiometric operating conditions at a combustor inlet total pressure level of 6 atmospheres (ref. 25). No smoke was detected when the combustor exit average temperature was below 1950 K. The smoke increases rapidly as the overall stoichiometric fuel-air ratio is approached. For comparison, the smoke number of the double-annulus combustor at an exit average temperature of 1500 K and the same operating conditions as for figure 20 is approximately 14. This illustrates the point that the fuel-air premixing that occurs in swirl-can combustors is a very effective way of reducing combustor smoke.

Air atomization. - One of the main advantages of air-atomizing fuel nozzles is their flexibility in design in producing fuel sprays which spread out fairly uniformly across the airstream. With improved atomization and mixing obtained from air-atomizing fuel nozzles, it would be expected that nitric oxide concentrations could be reduced (ref. 41). Besides being relatively simple in design and fabrication, air-atomizing fuel nozzles are less susceptible to fuel fouling at high inlet-air temperatures and require a relatively low fuel pressure drop as compared with the pressure-atomizing type. Thus, the use of air-atomizing nozzles appears promising as a means of reducing combustor exhaust emissions.

High-pressure-combustor exhaust emissions were determined by using low-fuel-pressure-drop air-atomizing nozzles designed to utilizing the airstream momentum in atomizing Jet A fuel (ref. 26). Similar tests were made with pressure-atomizing fuel nozzles for comparison. The air-atomization nozzles were first tested under ambient flow conditions in a full-scale Lucite model of the experimental combustor to determine

spray patterns produced with water injection. Photographs taken at several water-air ratios and reference velocities showed that a splash-cone type of air-atomizing nozzle gave a better distribution of liquid and a finer spray of water droplets than that obtained with a radial-jet type of air atomizer. As expected from water spray tests, radial-jet nozzles gave high smoke numbers in preliminary combustor tests. Thus, the splash-cone air-atomizing nozzle shown in figure 21 was selected for the combustor tests.

The fuel nozzle assembly shown in the figure consists of a diffuser snout in which a portion of the air from the compressor is captured and flows through the air swirler and around the splash-cone nozzle. The air swirler produces a rotating airflow which assists in evenly distributing the fuel droplets and stabilizing the subsequent flame. Low-pressure fuel is injected from the combination fuel supply and splash-cone support through four 0.16-centimeter-diameter orifices onto the curved face of the nozzle. Fuel splashes over the nozzle lip and is atomized by the swirling airstream. At the point where the airstream first contacts the fuel, the diffuser passage converges to accelerate the flow of the resultant fuel-air mixture, which is then suddenly expanded into the combustor by the diverging portion of the diffuser. The nozzle assembly can be used either singly or in combination to provide the required distribution for can combustors, can-annular combustors, or annular combustors.

A high-pressure-combustor segment 0.32 meter long with a maximum cross section of 0.153 meter by 0.305 meter was tested with the splash-cone air-atomizing and conventional simplex pressure-atomizing fuel nozzles (ref. 26) at inlet total pressures of 4 to 20 atmospheres, inlet total temperatures as high as 590 K, reference velocities of 12.4 to 26.1 m/sec, and fuel-air ratios of 0.008 to 0.020. Pollutant emissions obtained with the splash-cone air-atomizing nozzle configuration are compared with results obtained with pressure-atomizing fuel nozzles. Most of the results to be described herein were obtained at an inlet total temperature of 590 K, a reference velocity of 21.4 m/sec, and a fuel-air ratio of 0.015.

The variation of the NO_x emission index with pressure is shown in figure 22. Emission index generally increased with increasing inlet total pressure. However, there was a considerable drop in emission index with the splash-cone nozzle when inlet total pressure was increased from 10 to 20 atmospheres. This was attributed to improved atomization of the fuel when airstream momentum was increased. In this case, momentum was increased by increasing the airstream density. Thus, at an inlet total pressure of 20 atmospheres, the NO_x emission index was considerably lower with the splash-cone air-atomizing nozzle than with the pressure-atomizing nozzle. These tests were conducted with a fixed air-entry-hole geometry. It is conceivable that further reductions in oxides of nitrogen might be attained by adjustments in liner airflow distribution. Thus, from these data and data given in reference 42, it is judged that reductions in NO_x of the order of 30 percent may be obtained with air-atomizing fuel nozzles.

Increasing inlet total temperature gave a marked increase in the oxides-of-nitrogen emission index, as shown in figure 23. These data (unpublished data obtained by R. D. Ingebo and C. T. Norgren, NASA Lewis Research Center) were obtained with splash-cone nozzles similar to that shown in figure 21. Data from reference 26 are included in figure 23. This comparison shows that increasing the primary-zone equivalence ratio from approximately 0.63 to 4.50 substantially decreased the NO_x emission index.

Increasing combustor inlet total pressure from 4 to 10 atmospheres increased exhaust smoke numbers for all the fuel nozzles that were tested. However, smoke number decreased slightly with the splash-cone nozzle when inlet total pressure was increased from 10 to 20 atmospheres. As previously mentioned, nitric oxide (NO) emission index decreased in a similar manner, which was attributed to improved fuel atomization when airstream momentum was increased. Thus, with the air-atomizing splash-cone nozzle, an improvement in fuel atomization at high inlet total pressure tended to counteract the general tendency of smoke number to increase with increasing inlet total pressure. However, at 20 atmospheres, the splash-cone nozzle had a smoke number of about 35, somewhat higher than one of the pressure-atomizing nozzles tested but lower than that of another. It should be noted that the inlet total temperature of 590 K was somewhat below the design "takeoff" condition of 20 atmospheres and 755 K. Thus, smoke numbers are somewhat higher than might be expected at the design takeoff condition since increasing inlet temperatures tends to reduce smoke number.

Increasing either combustor inlet total pressure or temperature decreased CO and unburned total hydrocarbon emission indexes with both the splash-cone and pressure-atomizing nozzles. The comparison between the splash-cone and pressure-atomizing nozzles indicated that both CO and unburned total hydrocarbons were lower with splash-cone nozzles at an inlet total temperature of 589 K over a pressure range of 4 to 20 atmospheres although the combustion efficiencies for both fuel nozzles were near 100 percent. Initial results for the air-atomizing splash-cone fuel nozzle are promising, but a great deal more research is required to attain further reductions in oxides of nitrogen and smoke and to evaluate combustor durability and altitude relight capabilities.

Fuel prevaporization. - The injection of prevaporized fuel into a swirling airstream to obtain a homogeneous mixture of fuel and air can reduce NO_x concentrations in the reaction zone by producing a more uniform temperature profile than that obtained with liquid fuel injection. Prevaporization also eliminates the process of fuel droplet evaporation, thereby reducing the reaction-zone dwell time and NO_x emissions. However, operating a combustor with prevaporized Jet A fuel would require a heat exchanger to vaporize the liquid fuel prior to injection into the reaction zone. Thus, in order to meet heat-exchanger weight limitations, it would be advantageous to operate the combustor with partially vaporized fuel over a limited range of flight conditions.

One of the objectives of the tests described in reference 43 was to determine emis-

sion levels with varying degrees of vaporization. Vaporized propane was used to simulate vaporized kerosene. Propane was chosen to eliminate the complexities of operating a liquid fuel boiler and because its burning characteristics are similar to those of kerosene. Two different multiple-orifice fuel nozzles were used to inject varying proportions of liquid Jet A fuel and gaseous propane into the test combustor, as shown in figure 24. The experimental combustor that was used is similar to that described in the previous section. At a given fuel-air ratio, the summation of the mass flow rates for liquid Jet A and gaseous propane was held constant as the proportion of gaseous propane was varied from 0 to 100 percent. Fuel injector 1 consists of a simplex nozzle located in the center of the assembly for injecting liquid kerosene and a series of eight evenly spaced holes concentric with the simplex orifice for injecting gaseous propane. Fuel injector 2 is a commercial duplex nozzle in which the center orifice was used for injecting liquid kerosene and the annular orifice was used for injecting gaseous propane into the primary swirler air. The tests described herein were conducted over a range of inlet pressure and temperature of 4 to 20 atmospheres and 475 to 700 K, respectively, a fuel-air ratio of 0.014, and a reference velocity of 21.3 m/sec.

Figure 25 shows the variation in the NO_x emission index with combustor inlet total temperature for varying proportions of gaseous propane. The results obtained with fuel injector 1 indicate that as the inlet temperature is increased from 478 to 700 K, the emission index for oxides of nitrogen increases from 5 to 22 for 0 percent vapor. The effect of vapor fuel on the NO_x emission index is negligible to an inlet temperature of about 590 K. The reduction in NO_x that occurred as the proportion of vapor fuel was increased became more significant as inlet temperature was increased further. At 700 K, a considerable improvement was obtained, amounting to a 22 percent decrease in NO_x, as the proportion of vapor was increased from 0 to 100 percent. The results obtained with fuel injector 2 were similar, with the exception that the general level for the NO_x emissions was lower.

Figure 26 shows the variation in smoke number with combustor inlet total pressure for varying proportions of gaseous fuel. As inlet pressure was increased from 4 to 20 atmospheres, the smoke number for fuel injector 1 increased from 12 to 27 with 0 percent vapor. At a pressure of 20 atmospheres, increasing the proportion of vapor from 0 to 100 percent decreased the smoke number by 51 percent. Fuel injector 2 produced a marked increase in smoke number as pressure was increased.

Fuel injector 1 displayed a higher level for the NO_x emission index but a lower level of smoke number than injector 2. The observed differences are attributed to differences in degree of fuel-air mixing between the two configurations. It appears that fuel injector 2 had less mixing, causing it to operate at locally fuel-rich conditions thus producing more smoke but lesser amounts of NO_x. No attempt was made to alter reaction-zone airflow distribution in these tests. The results indicate, however, that further reduc-

tion in NO_x might be obtained by improvements in fuel-air mixing (premixing) or by adjusting the amount of primary-zone airflow.

Although the combustor operated at combustion efficiencies approaching 100 percent for all test conditions described herein, the emission index for CO still decreased significantly as the proportion of vapor increased from 0 to 100 percent, as shown in figure 27. The corresponding emission indices for total hydrocarbons were negligible for all test conditions.

Fuel-air premixing. - In the conventional turbojet combustor, liquid fuel is sprayed directly into the primary zone to give a mean fuel-air ratio near stoichiometric. Combustion is initiated and stabilized in this zone. Some reactions can continue in the secondary zone, where dilution air is admitted to bring the combustion temperature down to the level required at the turbine inlet. The injection of fuel in a spray results in a wide variation of local fuel-air ratio with a spectrum of locally lean to locally rich values. Because nitric oxide formation is exponentially dependent on local flame temperature, this distribution of stoichiometries results in large quantities of NO being produced in some regions and virtually none in others even for overall primary-zone fuel-air ratios far from stoichiometric. Thus, NO concentration cannot easily be predicted from the average reaction-zone fuel-air ratio in a conventional combustor with a nonuniform mixture.

For a premixed, prevaporized fuel system, on the other hand, the fuel-air ratio may be made uniform throughout the primary zone; the result is a very strong dependence of NO concentration on stoichiometry. Heywood, Fletcher, and Pompei (refs. 44 to 46) have studied the effect of primary-zone uniformity on NO production. Their work was based on a statistical evaluation of the equivalence ratio distribution in the primary zone. A crossplot of some of the typical analytical results from Fletcher and Heywood (ref. 44) is shown in figure 28, where the strong effect of uniformity on NO concentration can be seen. It is apparent from figure 28 that for a lean, uniformly mixed primary zone, significant reductions in NO concentration could be realized compared with conventional combustors operating near stoichiometric conditions.

The reactions responsible for the formation of NO are relatively slow compared with the other reactions which define the combustion process. Therefore, the concentration of NO is also strongly dependent on the residence time of the hot gases in the combustor. Since a premixed configuration requires less time for fuel vaporization and fuel-air mixing within the primary zone than a conventional combustor, it should be possible to decrease the hot-gas residence time by decreasing the combustor length for a premixed system.

Although a lean premixed primary zone will result in lower concentrations of nitric oxide compared with those from a conventional combustor, combustion stability can be expected to suffer. The lean flammability limit for most hydrocarbon fuels is about

50 percent of stoichiometric. In a nonuniform system, however, the mean fuel-air ratio can be considerably less than the lean limit, and locally rich zones will maintain combustion. For the uniform system which results from premixing, this advantage is lost and blowout will occur near the lean flammability limit.

A research program (ref. 47) was conducted to determine the effect of premixing on NO formation for conditions applicable to turbojet combustors. A 10-centimeter-diameter flame-tube combustor burning premixed gaseous propane fuel was used. The flame was stabilized with a drilled-plate which provided a total pressure drop of 4 percent of the upstream total pressure, a value typical of that in a turbojet combustor. Inlet conditions were maintained at a temperature of 590 K and a pressure of 5.5 atmospheres; the reference velocity was 23 m/sec. Concentrations of NO, CO, CO_2, and unburned total hydrocarbons were measured at a point 0.46 meter downstream of the flameholder for a range of fuel-air ratios from lean blowout to slightly rich. Combustion was stable for the present test conditions at an equivalence ratio φ as low as 0.54. Equivalence ratio φ is defined as the quotient of the fuel-air ratio of a given mixture divided by the stoichiometric fuel-air ratio. For leaner mixtures the combustion zone became unstable until blowout occurred at $\varphi = 0.5$. The fuel-rich combustion limit was not investigated.

Oxides-of-nitrogen emissions: Previous studies have shown that NO concentrations are generally of the order of 10 percent less than NO_x concentrations (ref. 23). Thus, measured values of NO shown in figure 29 (ref. 44) may be assumed to be approximately 90 percent of the actual NO_x values. By convention, NO concentrations are expressed as emission index (g NO_2/kg fuel), which is obtained by multiplying the NO emission index (g NO/kg fuel) by the ratio of molecular weights of NO_2 to NO. Equilibrium NO concentrations are included in figure 29 for comparison. Also given are the concentrations predicted at $\varphi = 1$ by well-stirred-reactor and well-stirred-reactor-plus-plug-flow analytical solutions. The former used the model of Edelman and Economos (ref. 48) with a reactor volume of 344 cubic centimeters; this is equivalent to assuming that the recirculation zone extends about 4.2 centimeters downstream from the flameholder. The results of this analysis were used as input to a plug-flow program to determine the effect of continued reaction for a distance of 42 centimeters, that is, the distance to the gas sampling probe in the test combustor.

The experimental data show the strong dependence on equivalence ratio that can be expected from premixed, prevaporized operation. For the combustor inlet total temperature used for the present tests (590 K), it was possible to obtain emission indices of less than 1 g NO_2/kg fuel for equivalence ratios less than 0.57. This compares with a minimum emission index of about 2 g NO_2/kg fuel from an experimental combustor designed for low NO_x (ref. 23) operating at about the same inlet conditions but with the advantage of a quick quench after a very short primary zone. Values for more conven-

tional combustors are in the range of 3 to 5 g NO_2/kg fuel for these inlet conditions.

The strong effect of residence time on NO concentration can be seen by comparing the well-stirred-reactor and well-stirred-reactor-plus-plug-flow analytical solutions. At $\varphi = 1$, these results predict that an order of magnitude increase in NO concentration results during the time the hot combustion products flow from the end of the reaction zone to the probe (about 4 msec). It is likely that the NO concentrations near the flameholder are significantly less than those reported herein, even for regions where the combustion is essentially complete. In a practical combustor, rapid quenching of combustion reactions by dilution air introduced at the end of the recirculation region could prevent concentrations from growing to the levels measured in this study. For this reason, the emissions from a practical premixing combustor could be lower than the values reported herein and might approach the concentrations predicted by the well-stirred-reactor solution.

Carbon monoxide, hydrocarbons, and combustion efficiency: Figure 30 shows that the measured CO concentrations were essentially at the equilibrium level for the entire range of equivalence ratio covered. The measurements of unburned total hydrocarbons showed concentrations less than 0.4 g CH_2/kg fuel over the entire span of stoichiometries investigated. Such values indicate combustion efficiency greater than 99 percent for all test points.

Heated fuel. - Using aircraft fuel as a heat sink for supersonic flight may affect the engine's exhaust gas emissions. The formation of NO is sensitive to flame temperature, which would be expected to increase with increasing fuel temperature.

Tests were conducted with natural-gas fuel over a range of combustor operating conditions to determine the magnitude of the effect of increased fuel temperature on the formation of NO_x. The data were correlated to a constant pressure of 6 atmospheres, a reference Mach number of 0.065, and zero inlet air humidity. The results are shown in figure 31, plotted on semilog coordinates for fuel temperatures from 300 to 800 K. The NO_x emission index increases with increasing fuel temperature at approximately a constant exponential rate. The rate of increase, however, is not as high as would be expected from theoretical calculations of the increased flame temperature and its effect on the rate of formation of NO_x.

Limited data were taken with heated Jet A fuel at simulated cruise conditions. The results are shown in figure 32, along with the results obtained with natural gas from figure 31. The overall level of NO_x emission is higher for Jet A fuel, but the rate of increase of NO_x with increasing fuel temperature is about the same for both fuels. This similarity is not surprising since the enthalpy variations of the two fuels over the same temperature range are about the same. These data show the effect of heated fuel on NO_x emission index for a specific combustor. They do not show the variations that might be expected from changes in combustor geometry and fuel-injection techniques.

Substitute Fuels

Alternate fuels that might be considered for future jet engines include fuel derived from shale oil or coal, liquefied natural gas (LNG), and hydrogen.

Fuel derived from shale oil or coal. - In principle, jet fuels could be produced from shale oil or coal that simulate, in all important respects, those presently derived from petroleum. In practice, there may be limits based upon cost and practical production yield of a synthetic fuel. Within these constraints, various options will be available. These options will comprise choices as to mode of production of initial crude from either shale oil or coal plus choices of the subsequent treatment to produce turbine-grade fuel, especially in regard to the degree of hydrogenation and removal of nonhydrocarbon impurities.

Fuels derived from coal generally have a higher aromatic content than fuels derived from petroleum. A higher aromatic content may increase the quantity of soot in the engine exhaust; however, the aromatic content could be reduced by hydrogenation. It will be necessary to examine the benefits and penalties involved in broadening current aviation turbine fuel specifications since broader fuel specifications may result in a greater yield. Combustor research will be required to determine the feasibility of using these synthetic fuels in current jet engines and to determine if design changes will be required to accommodate the new fuel. Nevertheless, the cruise emission characteristics of fuels derived from coal or shale oil would not be expected to differ greatly from fuels derived from petroleum.

Liquefied natural gas. - The use of LNG as the fuel for engines powering a supersonic transport has many potential advantages over the use of the conventional kerosene fuels (refs. 49 to 52). The more important of these potential advantages are the increased heat-sink capability of LNG, its higher heating value on a weight basis, its low flame radiation, and the low smoke levels in the engine exhaust. As a result of this interest, many combustor programs were conducted to document the performance attainable with natural-gas fuel (refs. 53 to 59). These programs included combustors designed specifically for natural-gas fuel as well as combustors designed for use with kerosene fuel (Jet A). As expected, combustor performance with natural-gas fuel was equal to that obtained with Jet A fuel at combustor conditions simulating takeoff and cruise operation. However, combustor performance at off-design conditions was considerably poorer with natural-gas fuel. Combustion efficiency decreased markedly with decreasing pressure and was particularly sensitive to a decrease in the inlet total temperature. Of particular importance were the very poor altitude blowout and relight limits obtained with natural-gas fuel. For every operating condition, the measured blowout and relight pressures were significantly higher than those obtained with Jet A fuel (ref. 53).

The single-annular combustor of reference 39 has been tested with natural-gas fuel. Reference 60 gives details of the work done to determine an optimum method of injecting natural-gas fuel. Natural gas does not display stable combustion over as wide a range of operating conditions as conventional kerosene fuels in spite of the higher heating value of natural gas. The narrow combustible limits and high chemical stability account for the poor performance of natural-gas fuel at off-design engine operating conditions (refs. 61 and 62).

Liquefied natural gas does have an advantage over kerosene fuels in its well-documented tendency to produce lower emissions of NO_x (ref. 63). Figure 33 compares the emissions of NO_x for Jet A fuel and natural-gas fuel over a range of inlet total temperatures. Exit temperature was constant approximately 1500 K, combustion efficiency was approximately 100 percent, and test pressure was 6 atmospheres. In general, the use of natural gas resulted in approximately a 50 percent reduction in NO_x emissions.

Hydrogen. - Reference 64, summarized herein, compares the predicted exhaust pollutant emissions, characteristic of future subsonic and supersonic commercial aircraft, when either hydrogen or kerosene (JP) fuel are used. The potential of liquid hydrogen as a jet fuel for high-altitude aircraft is discussed in detail in reference 65. Extensive research was performed in the mid-1950's at NASA Lewis Research Center to adapt the use of hydrogen fuel to gas turbine engines for high-altitude aircraft (ref. 66). Considerable experience was gained with hydrogen both in the modification of existing combustors designed for using kerosene fuel and in the generation of combustor technology that utilized hydrogen's unique combustion properties (refs. 66 to 71).

The use of hydrogen fuel would obviously eliminate all CO, SO_2, hydrocarbons, and smoke contributed by aircraft using kerosene fuel. Therefore, attention is focused on the relative quantities of NO_x generated by using either fuel. Combustion properties of hydrogen and kerosene fuels are examined to indicate and compare their potential for minimizing NO_x emissions. Also, emission data are compared for hydrogen, Jet A, and propane fuels tested in an experimental combustor segment at simulated engine cruise conditions.

The combustion properties of hydrogen are discussed in detail in references 66 and 72. Hydrogen has a heating value (mass basis) that is approximately 2.75 times greater than that of JP fuel. The stoichiometric fuel-air ratios for hydrogen and JP fuel are 0.029 and 0.067, respectively. The heat-sink capacity of liquid hydrogen could be used for cooling hot components in the engine (ref. 52); therefore, hydrogen could be introduced into the combustor as a gaseous fuel. Two properties of any fuel that characterize its potential performance in a gas turbine combustor are (1) flammability range and (2) burning velocity.

Flammability range: Hydrogen has a much wider flammability range than JP. At the lean limit, hydrogen has an equivalence ratio of about 0.1 to 0.2, compared to a

value of about 0.5 for kerosene-type fuels. The rich limit for hydrogen occurs at an equivalence ratio of about 7, compared to a value of about 4 for kerosene.

Pressures above 1 atmosphere do not have a significant effect on the flammable limits; however, increasing the initial mixture temperature widens the flammability range. The lowering of the lean limit and the raising of the rich limit are linear with increasing temperature. Regardless of the initial temperature, the flame temperature for hydrogen burning in air is 1000 to 1100 K at the lean limit and 1200 to 1300 K at the rich limit (ref. 72). The flame temperature for kerosene would be expected to be about 1900 K at the lean limit and 1200 K at the rich limit.

From the viewpoint of combustor performance, a wide flammability range enhances combustion stability over a wide range of required engine operating conditions that include a large span in fuel flow rate. In the past, combustor engineers have designed gas turbine combustors with the primary zone operating near an equivalence ratio of unity at cruise or takeoff conditions. The formation of nitrogen oxides may be minimized by designing the primary zone (reaction zone) to operate at as low a flame temperature as possible. This may be accomplished by burning near the lean flammable limit within the primary zone. Since hydrogen has a wider flammable range than JP fuel, it has a greater potential for minimizing the formation of nitrogen oxides. As indicated previously, at their lean limit, the flame temperature is about 1000 to 1100 K for hydrogen and about 1900 K for JP. The flame temperature of hydrogen at its lean limit is lower than the required turbine inlet temperature for most engines. Therefore, the minimum reaction-zone equivalence ratio is somewhat above the lean limit. Furthermore, since hydrogen can be easily injected into the combustor as a gaseous fuel to provide a uniform mixture of fuel and air prior to combustion, a more even distribution of flame temperature may be achieved to approach a low NO_x formation rate.

Burning velocity: The laminar burning velocities for hydrogen and a typical hydrocarbon (propane) are compared in figure 34 for a pressure of 1 atmosphere and for an initial ambient temperature. The maximum burning velocity for hydrogen is shown to be about 8 times greater than the maximum value for propane. The maximum burning velocity for hydrogen, unlike that for propane, does not occur near an equivalence ratio of unity but instead occurs near a fuel-rich equivalence ratio of about 1.8.

The influence of pressure on burning velocity is not considered to be significant over the range of interest for gas turbine combustors (ref. 73). Burning velocity increases exponentially with increases in initial temperature. The effect of turbulence on burning velocity is not well documented; however, turbulent flames consume a mixture more rapidly than laminar flames (ref. 72).

The higher burning velocity for hydrogen is attributed to a higher reaction rate and to higher mass diffusivity and thermal conductivity. From the viewpoint of combustor performance, the higher burning velocity for hydrogen enables stable combustion to

occur at much more severe operating conditions (lower combustor inlet pressures and temperatures and/or higher velocities) than with JP fuel and introduces the possibility of completing combustion in a shorter length combustor. This is illustrated in figure 35, in which the space heating rates are compared for hydrogen and JP-4 fuel. The combustion properties of JP-4, described herein, are similar to either JP-5 or commercial-grade aircraft fuel (Jet A). The space heating rate is indicative of the minimum combustor volume required to complete combustion at a given fuel flow rate or heat release rate. The shaded region in the figure represents the spread of experimental data for both turbojets and ramjets. The space heating rate limit shown for JP-4 is based on data from a perfectly stirred reactor experiment (ref. 74) in which fuel-air mixing is nearly instantaneous. This limit is approximately one order of magnitude higher than has been measured in practical gas turbine combustors, which are limited by the rate of mixing. The limit shown for hydrogen was estimated from the ratio of the burning velocities for hydrogen and hydrocarbon fuels. The higher theoretical space heating rate for hydrogen suggests that a much shorter primary zone would be adequate for completing combustion. A shorter combustor is desirable from the viewpoint of reduced engine weight. Reductions in primary-zone dwell time possible with hydrogen could result in a proportionate reduction in nitrogen oxide.

Experimental test data: Oxides-of-nitrogen emissions were measured at the exhaust of an experimental turbojet combustor segment using gaseous hydrogen fuel (ref. 75). The NO_x emissions obtained with hydrogen were compared with those obtained with both liquid Jet A fuel (similar to JP-5) and gaseous propane at similar combustor operating conditions. The experimental combustor used to obtain these data was not specifically designed as a low NO_x combustor; nevertheless, these data do indicate the trends and sensitivities of NO_x emissions with combustor operating conditions. The experimental combustor (fig. 24) employed to obtain these data had been previously used to study the effects of prevaporized fuel on exhaust emissions (ref. 27). The combustor segment, which had a width of 0.31 meter, a maximum height of 0.15 meter, and a length of 0.32 meter, utilized four multiple-orifice fuel injectors. Liquid Jet A fuel was injected through a simplex nozzle located in the center of the assembly, and either gaseous propane or gaseous hydrogen was injected through eight evenly spaced orifices surrounding the simplex nozzle. Primary airflow passed through an inlet snout and entered the combustor through swirlers surrounding the fuel injectors. Secondary air entered the combustor through holes and scoops in the liner wall. Gas samples collected at the combustor exit were analyzed for total NO_x by a chemiluminescence meter and include both NO and NO_2.

The effect of combustor inlet total temperature on total NO_x concentrations for the three different fuels is shown in figure 36 (ref. 64). The comparison is based on volumetric concentrations (ppm) rather than on the emission index. For the same combustor

temperature rise and airflow, only about one-third the fuel mass flow is required for hydrogen as for JP because of the higher heating value of hydrogen. Thus, since emission index is inversely dependent on fuel-air ratio, the emission index for hydrogen would be nearly three times as high as for JP for the same volumetric exhaust concentration. *Thus, volumetric concentrations (ppm) offer a more realistic basis for comparing* emissions of hydrogen with that of JP-type fuels.

The combustor temperature rise ΔT was held the same for all three fuels, combustor inlet total pressure was 4 atmospheres for hydrogen and 10 atmospheres for both liquid Jet A and propane; however, to provide a comparison for the fuels, the 10-atmosphere data were corrected analytically to values equivalent to 4 atmospheres by using a square-root-of-pressure correction. The NO_x concentration levels for JP fuel, corrected to a pressure of 4 atmospheres, were nearly identical to the NO_x concentration levels for hydrogen. From airflow distribution calculations, the primary-zone equivalence ratios were estimated to be about 0.75 for JP and 0.43 for hydrogen.

Several different primary-zone equivalence ratios were tested with hydrogen by adjusting the primary-zone airflow distribution. These results are shown in figure 37 as NO_x concentration plotted against flame temperature (ref. 64). The flame temperature was calculated for each primary-zone equivalence ratio by assuming equilibrium conditions. The observed rate of reduction in NO_x with decreasing flame temperature is not as great as expected from theory, which may be attributed to the fact that mixing uniformity was not optimized.

Experimental Clean Combustor Program

The goal of this program is to develop and demonstrate technology to decrease pollutant emissions of modern gas turbine engines (ref. 22). This technology is mainly applicable to advanced CTOL aircraft with engine compressor pressure ratios of approximately 20 to 35. However, the combustor technology generated will also be applicable to engines for supersonic aircraft. The program will be conducted in three phases. Contracts for the first phase were recently awarded by NASA Lewis Research Center to both General Electric and Pratt & Whitney Aircraft. In this first phase of the program, both contractors will conduct experiments in combustor test facilities to screen combustor concepts for reducing emissions. Each contractor will evaluate the Lewis swirl-can concept in addition to several of their own concepts. The primary emphasis of these contracts will be to demonstrate a reduction in NO_x emissions to approximately one-fourth of the current levels for production engines. There is also a requirement to significantly reduce emissions at engine idle conditions. Addendums to this program have also been included to reduce the NO_x emission index to a level of 5 g NO_2/kg fuel during cruise for supersonic commercial aircraft.

In the second phase of the program, further tests will be conducted to develop the best designs of phase I and to demonstrate satisfactory combustor performance, including uniformity of exit temperature profile, altitude ignition capabilities, and durability. In the third program phase, the best combustor concepts will be evaluated in a demonstration test of a high-compressor-pressure-ratio engine. This technology may be available to engine designers during the 1980-85 time period.

Combustor designs. - Figures 38 to 44 are cross-sectional sketches of the various combustors being tested. Figure 38 is a sketch of a two-row swirl-can combustor installed in a CF6-50 combustor passage. Combustors consisting of 60, 72, and 90 modules will be tested. Figure 39 shows a three-row swirl-can combustor consisting of 120 modules of varying diameter mounted in a JT9D combustor. Each row contains 40 modules. Each contractor will study swirl-can combustors by evaluating many variations in swirler, flame-stabilizer design, fuel-injection techniques, and airflow through the swirl can.

Figure 40 is a sketch of the fully premixed combustor designed for the JT9D engine. This combustor consists of two premix passages. The primary burner supplies all power during engine idle operation. Both burners are employed for operation at higher power levels. Another version of a staged premix combustor is shown in figure 41. This combustor, designed for the CF6-50 engine, uses a pressure-atomizing nozzle in the primary passage and employs premixing in only the secondary or full-power passage. Figure 42 is a sketch of a modified CF6-50 combustor that incorporates a pressure-atomizing fuel nozzle and a high dome airflow rate such that the entire primary zone operates at a low overall value of equivalence ratio. Variable geometry will be simulated with this combustor by varying the primary and secondary airflow splits. Figure 43 is a sketch of a swirl-type combustor designed for the JT9D engine. In this combustor concept, combustion is initiated in the pilot combustion zone, which is the only zone operating at idle conditions. For higher power operation, fuel is added through the secondary fuel injectors, and combustion occurs in the secondary combustion zone. The NO_x emissions may be minimized by the intense stirring caused by air admitted to this zone through rows of secondary air swirlers. The final combustor configuration being investigated is a double-annular combustor designed for use in the CF6-50 engine and shown in figure 44. This configuration employs the lean-dome concept similar to the one shown in figure 42. The use of a double-annular concept allows for radial staging of the fuel during idle operation, while the overall fuel lean primary zones should result in low NO_x emissions at full-power operation.

Augmentors

As indicated in a previous section, neither afterburners nor duct burners would be

expected to be significant contributors of CO, hydrocarbons, or NO_x emissions. No definitive program to reduce augmentor emissions has been undertaken at this time. Nevertheless, should reductions in emission levels be required, much of the technology being generated for combustors could be applied to both duct burners and afterburners.

The utilization of fuel staging and/or variable geometry, as proposed in reference 7, might be expected to result in increased combustion efficiency and reduced emissions. However, augmentors have traditionally been found to be more prone to combustor pressure oscillations (combustor instability) as design modifications are incorporated to increase combustion efficiency.

Reference 7 provides combustion efficiency data for an experimental full-scale duct burner. These data are shown in figure 45 as a function of a ramjet correlation parameter $P^{0.3}T/V_r^{0.8}$. The terms P, T, and V_r refer to the combustor inlet reference quantities of pressure, temperature, and velocity. Reference 76 utilized this parameter to correlate empirical data for a combustor employing V-gutter flameholders. (This parameter was found to provide a better fit to the duct-burner data than the correlating parameter P_3T_3/V_r described previously that is used for correlating combustor data.)

PROJECTED ENGINE CYCLES

For this study, engine designs were selected for both a subsonic and supersonic mission that resulted in minimum values of aircraft takeoff gross weight (TOGW) for a given payload and range and a specified noise constraint. Airplane economics are improved as TOGW is reduced. Takeoff gross weight varies as the engine design parameters (turbine inlet temperature, overall pressure ratio, fan pressure ratio, and bypass ratio) and engine size are varied. The values selected for these engine design parameters are influenced by the noise constraint which penalized TOGW. However, the values selected for these engine design parameters were not constrained by engine exhaust emission limits. It has been assumed that engine exhaust emissions would be minimized by means of low-emission combustor technology.

A reduction in the NO_x emission index might be achieved by lowering the overall pressure ratio below the values selected in this study, but this could not be done without penalizing TOGW. A moderate reduction in overall pressure ratio might be tolerable, but a large reduction in overall pressure ratio would seriously penalize TOGW. Similarly, a small reduction in NO_x might also be obtained by reducing the turbine inlet temperature, but, again, not without penalizing TOGW. For the supersonic mission, NO_x might be reduced by minimizing cruise flight speed. None of these emission constraints have been considered in this study.

Tables III and IV describe commercial aircraft systems and cruise operating conditions, respectively, for both subsonic and supersonic missions which are forecast for

the time period of 1980-85 and for 1990 and beyond. These forecasts are made on the premise that conventional JP fuel will continue to be the only aircraft fuel that is used extensively before 1990. The economics of using either liquid hydrogen or LNG as future aircraft fuels are discussed in reference 77. The replacement of conventional JP fuel by either hydrogen or LNG depends on many undecided factors that are beyond the scope of this report, such as future availability of fossil fuels and future production costs of synthetic fuels. There is no certainty at this time that either hydrogen or LNG will ever replace JP as an aircraft fuel. However, projected engine cycles using hydrogen or LNG have been included in this study based on the premise that the future use of these fuels is technologically possible. For the subsonic CTOL aircraft, it is assumed that production or growth versions of the 747 or DC-10 will continue to be in service to at least 1990 and that advanced turbofan engines using low NO_x combustor technology could be incorporated into these aircraft between 1980 and 1985. An Advanced Technology Transport (ATT) fueled by JP could be operational in the early 1990's, while advanced versions of the ATT fueled by either LNG or hydrogen might be a possibility in the late 1990's. For the supersonic mission, it is forecast that the Concorde would enter service in 1975 and that growth versions of the Concorde would remain in service to at least 1990. Detailed information is lacking on the TU-144, which is expected to become operational in 1974; however, its operating characteristics should be similar to those of the Concorde. A JP-fueled Advanced Supersonic Transport (ASST) might be operational in the early 1990's, while an ASST using either LNG or hydrogen might be possible in the late 1990's. The analytical data presented in tables III and IV for the future subsonic (ATT) and supersonic (ASST) aircraft are based on mission-analysis calculations (performed by James F. Dugan, Jr., of NASA Lewis Research Center) similar to those described in references 78 and 79, respectively. Although these mission analyses consider information and comments from aircraft engine and airframe manufacturers and airlines, they do not indicate any commitments that future aircraft and engines will match these predictions. These indicated engines and aircraft statistics are, however, the best information available to the authors at this time.

Advanced Technology Transport

An airframe with a supercritical wing was selected. At the design cruise conditions of Mach 0.85 and 12 200 meters altitude, the nominal lift-drag ratio L/D was 20. The design range was 5560 kilometers with a payload of 200 passengers for a transcontinental mission. An intercontinental mission with a design range of about 10 200 kilometers has also been considered but has not been included in table III since the combustor operating conditions do not differ greatly from those for the transcontinental mission and, thus, the exhaust emission indices would be similar. Takeoff gross weight of the ad-

vanced subsonic aircraft is about 113 000 kilograms with JP fuel, 102 000 kilograms with LNG, and 68 000 kilograms with hydrogen (about 0.6 of the takeoff gross weight using JP). Three high-bypass-ratio turbofan engines are specified for the advanced subsonic mission. The engines selected resulted in a noise level of 96 effective perceived noise decibels (EPNdB), which is 10 EPNdB below the Federal Air Regulation (FAR) 36 requirement. The bypass ratio during cruise is 7.8 with either JP, LNG or hydrogen. An advanced turbine cooling scheme (full-coverage film cooling) was assumed and as much as 13 EPNdB of fan machinery noise suppression. The total fuel flow rate per engine during cruise is 1610 kg/hr of JP, 1280 kg/hr of LNG, and 356 kg/hr of hydrogen.

Advanced Supersonic Transport

The duct-burning turbofan engines for the ASST were selected to meet an FAR 36 sideline noise constraint (108 EPNdB). Bypass ratio and fan pressure ratio were determined by considering the jet exit velocities (and hence jet noise) of the two streams, which, when added, produce 108 EPNdB without suppression. The engines were sized for a maximum dry (i.e., non-duct-burning) takeoff with acceptable field length and community noise requirements (at 6.5 km from start of roll). Turbine inlet temperature and cooling bleed were selected as being suitable for advanced full-coverage film cooling. For the cryogenic fuels (LNG and hydrogen) which may be used for turbine cooling, no benefit was detected by raising the turbine inlet temperature above that used with JP-fuel as long as the noise constraint was maintained. The airplane used in this evaluation cruised at Mach 2.7 at an altitude of 19 800 meters. Initial cruise altitude was optimized to maximize the quotient of L/D to specific fuel consumption (sfc). An L/D of 9.9 was typical for either the JP- or LNG-fueled airplanes, while a value of 7.5 was typical for hydrogen fuel. For either fuel, the cruise duct-burner temperature was reduced from the climb setting so that operation was near the minimum point on the sfc-thrust curve. A design range of 7400 kilometers was obtained in an all-supersonic-cruise mission (i.e., with no subsonic cruise leg) with 250 passengers. Takeoff gross weight for the ASST is about 382 000 kilograms with JP, 348 000 kilograms with LNG, and 229 000 kilograms with hydrogen. The cruise bypass ratio is 2.36 for either JP, LNG, or hydrogen. The combustor fuel flow rate per engine during cruise is 10 750 kg/hr of JP, 8700 kg/hr of LNG, and 2560 kg/hr of hydrogen (about 24 percent of the fuel flow rate using JP). A small degree of augmentation is require during cruise that results in a duct-burner fuel flow rate of 4200 kg/hr of JP, 3500 kg/hr of LNG, or 940 kg/hr of hydrogen (about 22 percent of the JP fuel flow rate). The total engine fuel flow rate during cruise is 14 950 kg/hr of JP, 12 200 kg/hr of LNG, or 3500 kg/hr of hydrogen (about 23 percent of the JP fuel flow rate).

PROJECTED COMBUSTOR TECHNOLOGY

There are a number of critical performance factors that must be considered in the design of any gas turbine combustor for an aircraft: combustion efficiency, total pressure loss, durability, exit temperature profile, and altitude relight. Combustor size and weight are important because they influence the overall weight of the engine. Combustor length affects the turbine shaft length and the bearing requirements. Reducing combustor length also reduces the amount of air required to cool the combustion liner by reducing liner surface area and may also be desirable for reducing NO_x emissions by reducing reaction-zone dwell time.

Proposed Federal regulations designed to control noise limits and air quality are expected to have a significant impact on the design of future aircraft engines (ref. 6). In order to offset the economic penalties of low noise, the engines must be lighter and more efficient, further emphasizing the requirement for compact engine components such as combustion systems.

Proposed regulations of aircraft emissions include limits on gaseous pollutants (CO, total hydrocarbons, and NO_x) which are produced during a defined landing-takeoff cycle (ref. 80). This cycle covers all aircraft operations below an altitude of 915 meters. A limit on smoke emissions sets a maximum value on the Society of Automotive Engineers (SAE) smoke number. Meeting these aircraft emission regulations requires that improvements be made in combustor design to reduce hydrocarbons and CO during engine idle and taxi and to reduce NO_x and smoke during takeoff. Many of the techniques being investigated to reduce NO_x during takeoff are also applicable to the reduction of NO_x during cruise; however, the techniques being studied to reduce CO and total hydrocarbons at engine idle by improving combustion efficiency during idle are generally not required for cruise conditions since the combustion efficiency is already near 100 percent at cruise. Some of the techniques used to minimize idle CO and total hydrocarbon pollutants may adversely affect the formation of NO_x or smoke at higher power conditions. Thus, future combustor designs might require variable geometry for the control of primary airflow distribution and/or fuel distribution to minimize pollutant formation over a wide range of engine operating conditions.

All these factors must be considered in arriving at the combustor technology requirements for the projected engine cycles included in table IV. The combustion efficiency during cruise of future combustors designed for either ATT or ASST aircraft should be virtually the same as for present production combustors, which is very near 100 percent. It may be feasible to design either turbojet afterburners or turbofan duct burners with combustion efficiencies near 100 percent during cruise by means of effective fuel atomization and fuel-air mixing. Optimum fuel-air mixing might be attainable by variable geometry to control airflow and/or fuel flow distribution. Significant in-

creases in combustor or augmentor total pressure loss cannot be tolerated because increasing these losses results in reductions in both engine thrust and specific fuel consumption.

Particular attention directed to the control of combustor durability and exit temperature profile will also be necessary because these factors affect the operating life of the hot engine components. Significant improvements in both materials and cooling methods may be required to maintain good combustor durability and exit temperature profile for future engines (table IV), which show a trend of increasing combustor exit temperatures.

Satisfactory reignition capabilities are required to allow startup of the engine in the event of a flame blowout at altitude. The technique of leaning-out the primary zone to minimize NO_x may adversely affect altitude relight; therefore, special procedures may be necessary to regain relight capabilities lost by design changes for reduced emissions.

The advantages and problems associated with the use of a cryogenic fuel such as LNG or hydrogen for jet aircraft are discussed in reference 52. Either fuel's heat-sink capacity may be used to cool hot engine components, and hydrogen's heating value (based on mass) is about 2.75 greater than for JP, while LNG's heating value is about 12 percent greater than for JP. These advantages are at least partially offset by the complications involved in having to store this fuel at a very low temperature and by the fact that the fuel has a lower density. A larger storage volume and insulated tanks are required.

Specific design approaches for minimizing exhaust emissions during cruise for the projected engines cycles of the future are discussed in this section. The discussion of combustor design techniques will accentuate those concepts that may effect a reduction in NO_x emissions during cruise operation. As indicated in table V, two levels of combustion system design changes for reducing cruise emissions shall be considered: (1) class 1 - minor retrofits to existing production engines or minor improvements to growth versions of these production engines, and (2) class 2 - major redesign (advanced state-of-the-art emission reduction technology) based on current experimental emission reduction programs such as the NASA Experimental Clean Combustor Program. For comparative purposes, emission limits determined by chemical kinetics calculations for a premixing-prevaporizing combustor are also included. The two levels of design improvement, in turn, represent increasing design complexity and a greater departure from conventional design methods, and the theoretical minimum represents a goal to strive for in practical combustor design by approaches that have not yet been determined.

It is judged that the technology required for a class 1 modification to a JP-fueled combustor should be available within 1 to 2 years; however, an additional 3 to 5 years would be required for implementing the modification and obtaining the necessary engine certification. Approximately 3 to 5 years should be required to evolve the technology

for a class 2 modification to a JP-fueled combustor. After demonstrating the class 2 technology, an additional 4 to 5 years should be required to implement this modification into an advanced engine design. An even longer time would be required to implement these modifications for either LNG- or hydrogen-fueled aircraft.

Table VI summarizes the projected combustor technology that might be used in the advanced propulsion systems listed in tables III and IV. Specific combustor concepts are based on a projection of the emission reduction technology described in this report. The predicted levels of design improvement, or "class change," are described in the following paragraphs.

Class 1 Engine Modification

The simplest modification to the combustor that may be envisioned would be a retrofit or redesign of the fuel-injection system to improve the atomization and carburetion of the fuel.

JP-fueled aircraft. - The concept of air atomization discussed in the section STATUS OF EMISSION REDUCTION TECHNOLOGY OF COMBUSTORS AND AUGMENTORS may be capable of providing a more uniform fuel-air mixture than is possible with the conventional pressure-atomized fuel injector. Air-atomizing fuel injectors are currently under evaluation in several engine development programs. Further research on air-atomizing fuel injectors is required to evolve designs that (1) operate well over a wide range of fuel flows, (2) demonstrate good durability, and (3) satisfy altitude relight requirements.

Liquefied-natural-gas-fueled aircraft. - Experience in the use of natural-gas fuel in stationary gas turbine engines already exists. Experimental research has also been performed in which vapor injectors were substituted for liquid-fuel injectors without altering the basic design of the conventional combustor (ref. 60). More research will be required to overcome the poor combustion stability characteristics of natural gas at off-design engine operating points. The use of natural-gas fuel in experimental combustors has been shown to result in significantly lower values of combustion efficiency at severe operating conditions, higher values of combustor pressure (lower flight altitude) for altitude ignition and blowout, and a stronger tendency for combustion instability than the use of JP fuel (ref. 62).

Hydrogen-fueled aircraft. - Past experience established by the NASA Lewis Research Center in the design and development of gas turbine combustors for hydrogen-fueled engines is described in references 66 to 71. Flight tests were conducted with a B-57 aircraft in which one of the production J65 turbojet engines was modified to accept gaseous hydrogen as well as JP fuel. The modification to the J65 combustor was rela-

tively simple and merely involved a change to the inlet fuel manifold. Similar modifications could be made to conventional combustors by substituting vapor injectors for existing pressure-atomizing swirl injectors and by redesigning the inlet fuel manifold to accommodate gaseous fuel.

Class 2 Engine Modification

A "class 2" change is defined as a major redesign of the combustor based on advanced emission reduction technology. Projections for the class 2 change will be based on swirl-can combustor technology. The swirl-can combustor described in detail in references 23 to 25 has no well-defined primary or secondary zones as does the conventional combustor. Nearly all the airflow, except for that required to cool the liner, passes directly through or around each element. The combustor can be shortened because of the rapid burning and mixing that occurs downstream of each element.

JP-fueled aircraft. - The multizone combustor concepts described in the section STATUS OF EMISSION REDUCTION TECHNOLOGY OF COMBUSTORS AND AUGMENTORS provide uniform reaction-zone temperature and a relatively quick quenching of the reaction by the dilution air. The swirl-can combustor is just one of the concepts being evaluated in the NASA Experimental Clean Combustor Program. Other types of low NO_x combustor concepts being investigated in this program may prove to be as attractive or even better than the swirl-can concept.

Liquefied-nautral-gas-fueled aircraft. - Experimental tests of swirl-can combustors designed specifically for natural-gas fuel are described in reference 57. Results obtained to date with natural gas in swirl-can combustors indicate that considerably more research and development will be required to improve combustor performance at off-design conditions.

Hydrogen-fueled aircraft. - The swirl-can combustor concept was initially conceived in 1956 with the objective of generating short-length combustor designs to take advantage of hydrogen's unique combustion properties (ref. 69). Figure 46 shows a quarter-sector test combustor that was used to simulate the performance of a full-annulus swirl-can combustor, together with the details of each swirl-can combustor element. Hydrogen fuel was injected tangentially into the combustor element and mixed with primary air entering the upstream orifice. An array of small V-gutters surrounding each combustor element provided flame spreading and interfacial mixing with secondary air passing around each element. Figure 47 shows an experimental full-annulus swirl-can combustor that was tested in a J65 engine using hydrogen fuel (ref. 66).

Theoretical Minimum Engine Emissions

Experimental research is just beginning in an attempt to evolve combustor concepts that may significantly lower the NO_x emission index to levels of the order of a factor of 10 below the current goals of the Experimental Clean Combustor Program. The NO_x emission projections for the premixed-prevaporized combustor presented herein will be based on the analytical calculations described here. The results of these calculations should be interpreted cautiously (1) because the analytical model used is an extreme simplification of the combustion process, (2) because additional improvements in the chemical kinetics equations that are used may be warranted as new chemical kinetics data become available, and (3) because the degree to which this theoretical result may be approached by practical combustor hardware is uncertain. Many problems may be envisioned in the evaluation of premixed-prevaporized combustors, including the design of a satisfactory vaporizer for JP fuel and the control of flashback.

The theoretical flame temperature is plotted against equivalence ratio for both hydrogen and JP fuel in figure 48. These data were obtained from the computer program of reference 81 for combustor inlet conditions (800 K, 5 atm) simulating supersonic cruise. The theoretical flame temperature for both hydrogen and JP reaches a peak at an equivalence ratio of about 1.1. For these inlet conditions, the maximum flame temperatures of hydrogen and JP are 2640 and 2560 K, respectively. The flame temperature for hydrogen is shown to be about 80 K greater than that for JP at identical conditions for equivalence ratios of 1 or less.

Oxides-of-nitrogen formation may be minimized by maintaining the lowest flame temperature possible in the reaction zone. Because of the lean flammability limit, the minimum flame temperature for hydrogen is shown to be about 1100 K (φ = 0.1) compared to a value of about 1900 K (φ = 0.5) for JP fuel.

Theoretical chemical kinetics calculations were performed to determine formation rates for NO by using the computer program of reference 82. A premixing-prevaporizing plug-flow reaction was assumed. These computations were initiated by using the equilibrium compositions calculated from reference 81 for both hydrogen and JP at an inlet temperature and pressure of 800 K and 5 atmospheres, respectively. Since combustion reactions were assumed to occur instantaneously, the calculated equilibrium compositions were used as the initial reactant concentrations, with the exception that the initial NO_x concentrations were set at zero. The NO producing reactions occurred at a constant reaction temperature equal to the equilibrium flame temperature for each given value of equivalence ratio. Since NO is the predominant oxide of nitrogen formed during combustion (substantially lesser amounts of NO_2 are also formed), the theoretical results will be limited to this particular species. A total of 24 intermediary kinetic reactions are considered in this computation, but the principal reactions forming NO are the

so-called Zeldovitch reactions between (1) monatomic oxygen and diatomic nitrogen and (2) monatomic nitrogen and diatomic oxygen.

The results of these computations are presented in figure 49 for a reaction dwell time of 2 milliseconds, which is representative of combustor primary zones. Nitric oxide emissions are shown here in terms of a volumetric concentration. Equilibrium NO concentrations are provided for comparison with the values limited by chemical kinetics. The NO concentrations determined by kinetics are significantly lower than the equilibrium concentrations because of the relative slowness of the NO formation reactions. At identical conditions, the NO concentration shown for hydrogen is slightly higher than that for JP because of the difference in flame temperature shown in figure 48. Figure 49 clearly shows the advantage of burning in the primary zone at as low an equivalence ratio as possible to minimize the formation of NO. Reductions might also be possible with a two-staged combustor by first burning fuel rich and then burning the remaining fuel at a lean equivalence ratio after uniformly mixing in additional air.

The lowest NO concentration attainable by burning with a lean fuel-air mixture in the primary zone is determined by the lowest practical primary-zone equivalence ratio. Emission characteristics of an experimental premixing-prevaporizing propane burner were reported in reference 47. Results presented in reference 47 for an inlet temperature of 590 K indicate that combustion instabilities occurred for reaction-zone equivalence ratios less than 0.54. To be conservative, a minimum primary-zone equivalence ratio of 0.6 was assumed for either JP or LNG fuel to ensure stable combustion. For hydrogen, the minimum primary-zone equivalence ratio is determined by the combustor overall fuel-air ratio (combustor temperature rise) and the proportion of air required for combustor cooling. On this basis, minimum primary-zone equivalence ratios of 0.4 and 0.45 were calculated for hydrogen for the ATT and ASST engines, respectively. About 10 to 20 percent of the combustor airflow is allocated for cooling. The results of these computations are shown for JP, LNG, and hydrogen in figure 50, in which NO concentration is plotted against combustor inlet total temperature for a reaction-zone dwell time of 2 milliseconds and combustor inlet total pressures of 5 and 10 atmospheres. Within the limits of the theoretical model used to perform the theoretical computations, these results provide only a preliminary indication of the ultimate minimum NO concentrations possible with these fuels. Practical combustor considerations such as the degree of mixing and the uniformity of the reaction temperature may significantly increase these theoretical estimates. In any event, from a theoretical point of view, hydrogen has considerably more potential for minimizing the NO concentration than JP fuel because of its lower lean flammable limit, its higher flame velocity, and its ability to produce a more uniform fuel-air mixture as a gaseous fuel.

Figure 51 provides an indication of the accuracy of the plug-flow model used in these predictions. The model was based on the assumption that all species, except the oxides

of nitrogen, have reached equilibrium in the hydrocarbon reaction. It is apparent that for JP fuel at an equivalence ratio of 0.6 the NO concentration predicted is about an order of magnitude lower than the experimental value. However, the single data point at $\varphi = 0.5$ for the well-stirred-reactor model (ref. 83) which does not assume equilibrium hydrocarbon chemistry agrees well with the experimental results.

Within the reaction zone, the concentration of oxygen atoms can overshoot the equilibrium value by several orders of magnitude at low temperatures (ref. 48). Because the oxygen atom is an important part of the NO-producing scheme, a model which assumes equilibrium values cannot predict NO concentrations accurately. A recent study of premixed hydrogen flames also predicted NO concentrations lower than measured values when equilibrium levels of oxygen atom were assumed (ref. 84). For low-temperature flames, the difference between measured and computed concentrations was as great as an order of magnitude.

The model based on equilibrium hydrocarbon chemistry appears to be adequate for predicting NO concentrations for fuel-air mixtures near stoichiometric, perhaps because of the high reaction rates near stoichiometric which would minimize any effect of oxygen atom overshoot. Further modeling studies using the model of reference 83 are anticipated.

The rate of formation of NO is relatively slow compared with the hydrocarbon reaction rates; thus, the NO concentration is linearly dependent on hot-gas residence time. This study assumed a constant residence time of 2 milliseconds as being representative for present-day primary zones. Future technology may reduce this dwell time, thus resulting in a proportional decrease in NO concentration.

PROJECTED EMISSIONS

The projected engine exhaust emissions at cruise conditions are based on the advanced subsonic ATT and advanced supersonic ASST missions described in the section PROJECTED ENGINE CYCLES and table IV and on the use of JP, LNG, and hydrogen fuels. Projected emission levels are presented in terms of both an emission index (g pollutant/kg fuel burned) and an emission rate per engine (g pollutant/hr).

Emissions Affected Solely by Fuel Composition

The emission levels for constituents that are primarily affected by the composition of the fuel that is used are listed in table VII. In general, the emission indices for these constituents are independent of engine operating conditions. The variations in the emis-

sion indices for water and CO_2 shown in table VII for JP, LNG, and hydrogen are a function of the hydrogen-carbon ratio of each fuel. The hydrogen-carbon ratios (atomic) for JP and LNG were assumed to be about 1.94 and 4, respectively. Carbon formation within the combustor should only be prevalent with JP-type fuels. Despite the lack of quantitative data, the quantity of carbon in the exhaust during cruise should be quite small. The estimate for carbon was obtained from reference 1. The estimate for SO_2 was obtained from G. L. Brines of Pratt and Whitney Aircraft and is based on the current sulfur composition of commercial jet fuels. Total trace elements are defined to include metallic elements in the fuel in addition to a relatively smaller quantity of eroded metal from engine components. The estimate for total trace elements was obtained from Brines, as well as the estimate for the quantity of lubricating oil lost from the engine lubricating system.

Emissions Affected by Both Engine Operating Variables and Fuel Properties

The CO, total hydrocarbons, and NO_x emission forecasts presented herein for future commercial jet aircraft are based on the projected combustor technology described in the preceding main section. As has been discussed, these forecasts are divided into three categories of changes representing different levels of emission reductions. The first level, designated as a class 1 engine modification, assumes a moderate change or retrofit to existing combustion system designs. Emission forecasts for a class 1 change are based on current emission reduction research data for air-atomizing and vaporizing fuel injectors previously described. The second level, designated as a class 2 engine modification, assumes a complete redesign of the combustion system. Emission forecasts for a class 2 change are based on current experimental data for multizone combustors (swirl cans) described herein. The third level, designated as a theoretical minimum, represents the ultimate possible reduction in emissions. Theoretical minimum emissions are based on theoretical kinetics calculations for a premixed-prevaporized combustion system as described in the preceding main section. A class 1 change represents (1) the least alteration to the engine design; (2) a moderate reduction in emissions; and (3) the highest probability of being technically feasible without penalizing combustor performance. A class 2 change represents (1) a major redesign of the engine's combustion system; (2) a significant reduction in emissions; and (3) a medium probability of being technically feasible without penalizing combustor performance. To approach theoretical minimum emissions would mean (1) an extremely innovative redesign of the combustion system; and (2) a very low probability of being technically feasible without penalizing combustor performance.

For each level of change, the major motivation for the indicated modifications to

the engine's combustion system is to reduce NO_x emissions. Except for the case of the ASST duct burner, no reductions in the combustor's CO and total hydrocarbon emissions are projected below the best levels currently being observed for production engines because (1) these emissions levels are already quite low during cruise and (2) it is difficult to envision improvements in combustion efficiency of the core combustor, which is already as close to 100 percent as can be measured experimentally.

The use of alternate fuels such as LNG or hydrogen would not necessarily complicate the evolution of advanced low-emission combustion systems but would require significant technological changes to enable the storage and transfer of cryogenic fluids both for ground handling and aboard the aircraft. In fact, the ability to easily vaporize either LNG or hydrogen minimizes the effort required to develop a low-emission combustor. The future availability of these fuels or the future economics of their use have not been considered as an influential factor in these forecasts other than as they affect the possible projected time at which these fuels might be put into service as described in the section PROJECTED ENGINE CYCLES.

Procedures for NO_x emission index data extrapolations. - In many cases, it was necessary to extrapolate available experimental emission data for NO_x to the combustor or augmentor operating conditions specified for the advanced engines described in table IV. These extrapolations were performed to correct for the proper inlet and exit temperatures and inlet pressures for the engines in table IV by using the data correlation methods described in reference 16. Inlet pressures are adjusted to the proper levels by applying a square-root correction. An exponential adjustment is applied to the inlet temperature by using the correlating parameter e^{T/T_d}, where T is the inlet temperature (in K) and T_d is a constant correlating factor evaluated to be 288 in reference 16. Variations in exit temperature are adjusted by applying a linear correction. Velocity or dwell-time corrections were not used because the combustor velocities of the experimental data available were judged to be representative of the requirements for the combustion systems of table IV.

No attempt was made to correct for differences in inlet-air humidity between test facility conditions and conditions at cruise altitude. Reference 85 indicates that the NO_x emission index increases with decreasing inlet-air humidity at a constant exponential rate of e^{19H} (where H is the humidity in g H_2O/g dry air). Typical values of inlet-air humidity for combustor test facilities vary from 0.0007 to 0.006 g H_2O/g dry air; thus, the application of combustor test data to a near-zero humidity at cruise altitude results in an underestimation of the cruise NO_x emission index by 1 to 12 percent.

Baseline production engines. - Exhaust emission estimates during cruise for representative production engines for both subsonic and supersonic commercial aircraft are tabulated in table VIII. The cruise emission estimates for the JT9D engine are extrapolated from average takeoff emission indices for the JT9D given in reference 5. The

JT9D takeoff emission indices for CO and total hydrocarbons are judged to be representative of cruise emissions because the correlating parameter P_3T_3/V_r for either condition is high enough for the combustion efficiency to be independent of operating conditions (fig. 7). These emission indices for CO and total hydrocarbons are also used to characterize combustor emissions for the advanced engines tabulated in table IX. The emission rates shown in both tables VIII and IX are based on the fuel flow rates per engine listed in table IV.

Emission estimates for the Olympus 593 engine were obtained from reference 1 (pp. 173-179). The Olympus 593 engine does not use afterburning during steady-state cruise.

Class 1 engine modification. - Emission forecasts for a class 1 change for both an ATT and ASST mission are tabulated in table IX for JP, LNG, and hydrogen.

JP-fueled aircraft: The class 1 emission forecasts indicated for the ATT using JP are related to the operating requirements of the advanced turbofan engine (table IV) but should also be applicable to retrofitted production engines.

A reduction in the NO_x emission index of 30 percent below the baseline levels for the JT9D and Olympus 593 core engines given in table VIII is assumed on the basis of the availability of improved air-atomizing fuel-injector technology similar to that described herein. The NO_x emission estimates shown in table IX have also been corrected for differences in operating conditions (combustor inlet total pressure and temperature and combustor exit temperature) between the baseline and advanced engines. This correction for differences in combustor operating conditions results in an additional NO_x decrease of about 21 percent for the ATT combustor and an NO_x increase of 8 percent for the ASST combustor, relative to baseline conditions. This 21 percent reduction in NO_x for the ATT results mainly from the lower projected values for combustor inlet temperature and pressure (table IV(a)). The 8 percent increase in NO_x for the ASST is mainly the result of the higher projected value for combustor exit temperature (table IV(b)). Thus, the net reduction of the NO_x emission indices for the class 1 ATT and ASST combustors, relative to the baseline engines, is about 45 and 24 percent, respectively, as shown by comparing table IX(a) with table VIII.

The NO_x emission index for the ASST duct burner is estimated from the data of figure 16 for a single-annular primary combustor (corrected to duct-burner operating conditions). This approach is considered justifiable because the combustion characteristics of a duct burner should be similar to those of a primary combustor running at the same operating conditions. The projected NO_x emission rate for the duct burner results in an increase of less than 10 percent over the NO_x emission rate for the core engine.

The duct-burner combustion efficiency was estimated to be about 98 percent at the cruise operating conditions of table IV by extrapolation of the correlation curve of figure 45 and by assuming that duct-burner performance would be similar to that of the

geometry of reference 7 at a fuel-air ratio of 0.02. With these assumptions the duct-burner's contribution to CO and total hydrocarbons is significantly greater than the contribution from the core combustor.

LNG-fueled aircraft: The NO_x emission index of an ATT combustor equipped with a fuel vapor injector and using LNG is estimated from figure 33 to be about 39 percent lower than that of a conventional JP-fueled combustor operating at the ATT combustor inlet temperature (table IV(a)). This reduction in NO_x is assumed to be offset by an increase in the NO_x emission index of about 21 percent that results from the effect of fuel heating shown in figure 31. A fuel temperature of about 300 K is assumed to result from using the fuel to cool hot engine components. Thus, at the ATT operating conditions, the reduction in the NO_x emission index with LNG is about 26 percent compared to a reduction of 30 percent for JP (class 1). After correcting for the difference in operating conditions between the baseline and ATT engines (table IV(a)), the net reduction in the NO_x emission index is about 41 percent, as shown by comparing table IV(b) with table VIII.

Similarly, from figure 33, the NO_x emission index for an ASST core engine using LNG is estimated to be about 34 percent lower than that of a conventional JP-fueled combustor operating at the ASST combustor inlet temperature (table IV(b)). The increase in the NO_x emission index caused by fuel heating is estimated to be about 24 percent. Thus, the net reduction is about 18 percent. After correcting for differences in operating conditions, the NO_x emission index for the ASST class 1 engine is about 11 percent below that for the baseline engine. The NO_x emission index for the ASST duct burner using LNG is assumed to be the same as that for JP and, again, contributes less than 10 percent to the engine overall NO_x emission rate.

The CO and total hydrocarbon emission indices for LNG are assumed to be approximately the same as the corresponding class 1 values for JP for both the core combustors and the ASST duct burner, since combustion efficiencies are approximately the same for both fuels at cruise conditions (ref. 62).

Hydrogen-fueled aircraft: The NO_x emission index for the class 1 ATT engine using hydrogen is estimated to be about three times greater than that of the baseline engine using JP at identical operating conditions, or a factor of about 2.4 times greater if the effect of the difference in operating conditions between the baseline and ATT engines is included (table IV(a)). This estimate is based on the data of figure 36 which show that hydrogen had a volumetric NO_x exhaust concentration that was about 5 percent higher than JP for the same test combustor. The hydrogen emission index is about three times greater than the JP emission index at identical operating conditions because only about one-third the fuel mass flow is required for hydrogen as for JP due to the higher heating value of hydrogen. Similarly, the NO_x emission index for the ASST core engine is estimated to be about 2.8 times greater than that of the baseline value for JP at identical

operating conditions, or a factor of about 3 times greater if the effect of the difference in operating conditions is included (table IV(b)). The NO_x emission index for the ASST class 1 duct burner using hydrogen is estimated to be about 2.8 times greater than the estimate for JP and results in a NO_x emission rate for the duct burner that is about 5 percent of the overall NO_x emission rate for this engine.

Class 2 engine modification. - The NO_x emission forecasts for making a class 2 change in either the ATT or ASST engines as tabulated in table IX for JP, LNG, and hydrogen are based on present swirl-can combustor data (figs. 16 and 17) and goals set for the NASA Experimental Clean Combustor Program for JP fuel.

JP-fueled aircraft: An NO_x emission index of 6 was calculated for the ATT combustor using JP fuel by correcting values obtained from figures 16 and 17 to cruise operating conditions. This represents about a 45 percent reduction in the NO_x emission index as compared with class 1 engines (69 percent reduction compared with present baseline engines). Based on the NASA Experimental Clean Combustor Program goal of reducing NO_x emission indices by about one-fourth those of the baseline engines, a forecast value of 4 was obtained. Thus, a NO_x emission index between 4 and 6 is forecast for the ATT combustor using JP fuel. Similar calculations were made for the ASST combustor, which gave an NO_x emission index forecast between 5 and 9.

An improvement from 98 percent to 99 percent in duct-burner efficiency for the class 2 ASST engine is arbitrarily judged to be attainable by the introduction of variable geometry to control airflow and/or fuel flow distribution.

LNG-fueled aircraft: Experimental NO_x emission data for a swirl-can combustor using LNG are not available. The NO_x emission index for the class 2 combustors using LNG is estimated from the class 2 JP estimate by applying a further correction for vapor fuel, as presented in figure 33. With this approach, the NO_x emission indices for the class 2 engines using LNG are estimated to be 39 and 33 percent lower than the corresponding levels for the class 2 ATT and ASST engines, respectively, using JP. No increase in the NO_x emission index is included as a result of fuel heating (fig. 31) because it is considered that this effect may be offset by reducing reaction-zone dwell time. The ASST duct-burner emission indices for the class 2 engine using LNG are assumed to be identical to the estimates for the class 2 engine using JP.

Hydrogen-fueled aircraft: Experimental NO_x emission data for a swirl-can combustor using hydrogen are not presently available. These NO_x emission indices are estimated from the corresponding values for the class 2 engines using LNG by assuming that the NO_x ppm level for hydrogen is equal to that for LNG. Hydrogen's wide flammability limits and high burning velocity should enhance the design of a low NO_x combustor by reducing both reaction-zone equivalence ratio and dwell time.

Minimum engine emissions. - The minimum NO_x emissions forecasts for the premixing-prevaporizing ATT or ASST combustor as tabulated in table IX for JP, LNG,

and hydrogen are obtained from the theoretical kinetics data of figure 50. A tenfold range of values for the NO_x emission index is indicated for each fuel. The lower value in this range was obtained directly from figure 50, while the upper value was obtained by applying a tenfold correction to these values to account for the effect of "oxygen overshoot" indicated by the data of figure 51 and discussed in the section PROJECTED COMBUSTOR TECHNOLOGY.

The upper value shown in table IX(a) for JP represents a more conservative estimate of the minimum attainable NO_x emission index for the assumed minimum primary-zone equivalence ratio of 0.6 and assumed reaction-zone dwell time of 2 milliseconds. Combustor operation with a minimum primary-zone equivalence ratio lower than 0.6 or a reaction-zone dwell time lower than 2 milliseconds might be possible at high combustor inlet temperatures. The lower NO_x estimate (table IX(a)) might be attainable by operating with a minimum primary-zone equivalence ratio of 0.5. In any event, as discussed in the section PROJECTED COMBUSTOR TECHNOLOGY, these preliminary analytical results should be interpreted cautiously. Minimum NO_x emission indices could conceivably be estimated more accurately when more realistic computer models are evolved and when more fundamental experimental data of the type obtained in reference 47 become available. The ASST duct-burner emission indices for CO and total hydrocarbons are assumed to be equal to the emission levels for the primary combustor.

Effect of Variations in Cruise Altitude and Mach Number

The emission forecasts presented in table IX are based on the constant cruise operating conditions for the projected engines given in table IV. These forecasts may be adjusted to a varying cruise flight envelope such as presented in references 1 (pp. 169-172) and 86, by applying corrections for variations to combustor or duct-burner operating conditions. In general, the CO and total hydrocarbon emission indices for either the ATT or ASST primary combustor are not sensitive to normal variations in combustor operating conditions during cruise, such as presented in references 1 and 86. Significant increases in the CO and total hydrocarbon emission indices for the ASST duct burner may occur during transonic acceleration because of lower combustor inlet temperature and pressure; however, the quantity of fuel consumed during transonic acceleration is considered to be relatively small in comparison to the total quantity of fuel used during cruise. If required, the duct-burner combustion efficiency predictions presented in table IX may be corrected for varying operating conditions by using the correlation of figure 45.

Projected NO_x emission indices may be corrected for varying cruise operating conditions by applying the corrections described in the section Procedures for NO_x emis-

sion index data extrapolation. The largest correction to the NO_x emission index would be from variations in flight Mach number. The projected NO_x emission indices would be expected to decrease exponentially with decreasing combustor inlet temperatures as flight Mach number is reduced. Because of the large uncertainty of the forecasts presented in table IX, it is doubtful that cruise altitude and Mach number corrections would necessarily improve the accuracy of these emission index projections; however, large variations in cruise fuel flow rates will result in proportionate variations in the projected emission rates.

CONCLUDING REMARKS

Forecasts were made in this study by predicting technological advances in reducing exhaust emissions of future commercial aircraft operating at high-altitude cruise conditions. Emission characteristics for future jet engines that were selected for both subsonic and supersonic missions were based on minimizing the aircraft takeoff gross weight for a given payload and range and a specified noise constraint. High-bypass-ratio turbofan engines were specified for an advanced subsonic aircraft, and duct-burning turbofan engines were specified for an advanced supersonic aircraft.

It is anticipated that growth versions of many present-day aircraft will continue in service to at least 1990 and that advanced engines that use low NO_x combustor technology could be incorporated into the design of these aircraft between 1980 and 1985. Advanced subsonic and supersonic aircraft could become operational in the early 1990's. It appears quite probable that JP-type fuels will continue to be the main energy source for commercial jet aircraft until at least the late 1990's.

Minor combustor modifications implemented by technological advances made within the next 4 to 7 years could reduce the oxides-of-nitrogen (NO_x) emission index by approximately 30 percent. However, greater reductions will be needed to meet proposed clean-air standards. It is anticipated that major combustor redesigns to reduce NO_x emission indices by as much as 75 percent below those of current production engines might require 7 to 10 years for development and engine certification. Minimum emission limits determined from chemical kinetics calculations for a completely premixed-prevaporized combustor predict that even lower NO_x emission levels are theoretically possible. This theoretical minimum actually represents a goal to be approached in practical combustor design.

Lewis Research Center
National Aeronautics and Space Administration,
Cleveland, Ohio, December 6, 1973,
501-24.

REFERENCES

1. Broderick, A. J., ed.: Proceedings of the Second Conference on the Climatic Impact Assessment Program. DOT-TSC-OST-73-4, U.S. Dept. of Transportation, Mar. 1973.

2. Platt, M.; Baker, R. C.; Bastress, E. K.; Chng, K. M.; and Siegel, R. O.: The Potential Impact of Aircraft Emissions Upon Air Quality. Report No. 1167-1, Northern Research and Engineering Corp., 1971.

3. Anon.: A Study of Aircraft Gas Turbine Engine Exhaust Emissions. Aerospace Industries Association of America, Aug. 1971.

4. Sawyer, R. F.: Atmosphere Pollution by Aircraft Engines and Fuels. AGARD-AR-40, 1972.

5. Bogdan, Leonard; and McAdams, H. T.: Analysis of Aircraft Exhaust Emission Measurements. CAL-NA-5007-K-1, Cornell Aeronautical Lab., Oct. 1971.

6. Beheim, Milton A.; Cummings, Robert L.; Dugan, James F., Jr.; Feiler, Charles E.; Grobman, Jack S.; and Stewart, Warner L.: Subsonic and Supersonic Propulsion. Vehicle Technology for Civil Aviation: The Seventies and Beyond. NASA SP-292, 1971, pp. 107-156.

7. Branstetter, J. Robert; Juhasz, Albert J.; and Verbulecz, Peter W.: Experimental Performance and Combustion Stability of a Full Scale Duct Burner for a Supersonic Turbofan Engine. NASA TN D-6163, 1971.

8. Diehl, Larry A.: Preliminary Investigation of Gaseous Emissions from Jet Engine Afterburners. NASA TM X-2323, 1971.

9. Palcza, J. Laurence: Study of Altitude and Mach Number Effects on Exhaust Gas Emissions of an Afterburning Turbofan Engine. Rep. FAA-RD-72-31 (AD-741249), 1971.

10. Diehl, Larry A.: Measurement of Gaseous Emissions from an Afterburning Turbojet Engine at Simulated Altitude Conditions. NASA TM X-2726, 1973.

11. Forney, A. K.: Engine Exhaust Emission Levels. Paper 73-98, AIAA, January, 1973.

12. Childs, J. Howard; Reynolds, Thaine W.; and Graves, Charles C.: Relation of Turbojet and Ramjet Combustion Efficiency to Second-Order Reaction Kinetics and Fundamental Flame Speed. NACA Rep. 1334, 1957.

13. Jones, Robert E.; and Grobman, Jack: Desing and Evaluation of Combustors for Reducing Aircraft Engine Pollution. NASA TM X-68192, 1973.

14. Rudey, Richard A.: Aircraft Engine Pollution Reduction. NASA TM X-68129, 1972.

15. Grobman, Jack: Review of Jet Engine Emissions. NASA TM X-68064, 1972.

16. Niedzwiecki, Richard W.; and Jones, Robert E.: Parametric Test Results of a Swirl-Can Combustor. NASA TM X-68247, 1973.

17. Bahr, D. W.: Control and Reduction of Aircraft Turbine Exhaust Emissions. Symposium on Emissions from Continuous Combustion Systems. General Motors Research Lab., Warren, Mich., Sept. 1971, pp. 345-373.

18. Butze, Helmut F.: Methods for Reducing Pollutant Emissions from Jet Aircraft. NASA TM X-68000, 1971.

19. Bastress, E. K., et al.: Assessment of Aircraft Emission Control Technology. Rep. 1168-1, Northern Research and Eng. Corp., July 1971.

20. Norster, E. R.; and Lefebvre, A. H.: Effects of Fuel Injection Methods on Gas Turbine Combustor Emissions. Symposium on Emissions from Continuous Combustion Systems. General Motors Research Lab., Warren, Mich., Sept. 1971, pp. 255-278.

21. Grobman, Jack: Effect of Operating Variables on Pollutant Emissions from Aircraft Turbine Engine Combustors. NASA TM X-67887, 1971.

22. Jones, Robert E.: Advanced Technology for Reducing Aircraft Engine Pollution. NASA TM X-68256, 1973.

23. Niedzwiecki, Richard W.; and Jones, Robert E.: Pollution Measurements of a Swirl Can Combustor. NASA TM X-68160, 1972.

24. Niedzwiecki, Richard W.; Trout, Arthur M.; and Mularz, Edward: Performance of a Swirl-Can Combustor at Idle Conditions. NASA TM X-2578, 1972.

25. Niedzwiecki, Richard W.; Juhasz, Albert J.; and Anderson, David N.: Performance of a Swirl Can Primary Combustor to Outlet Temperatures of 3600^{o} F (2256 K). NASA TM X-52902, 1970.

26. Ingebo, Robert D.; and Norgren, Carl T.: High Pressure Combustor Exhaust Emissions with Improved Air-Atomizing Fuel Nozzles. NASA TN D-7154, 1973.

27. Norgren, Carl T.; and Ingebo, Robert D.: Effects of Prevaporized Fuel on Exhaust Emissions of an Experimental Gas Turbine Combustor. NASA TM X-68194, 1973.

28. Clements, T. R.: Effect of Fuel Zoning and Fuel Nozzle Design on Pollution Emissions at Ground Idle Conditions for a Double-Annular Ram-Induction Combustor. Pratt & Whitney Aircraft (NASA CR-120194), 1972.

29. Briehl, Daniel; and Papathakos, Leonidas: Use of an Air Assist Fuel Nozzle to Reduce Exhaust Emissions from a Gas Turbine Combustor at Simulated Idle Conditions. NASA TN D-6404, 1971.

30. Juhasz, Albert J.; and Holdeman, James D.: Preliminary Investigation of Diffuser Wall Bleed to Control Combustor Inlet Air Flow Distribution. NASA TN D-6435, 1971.

31. Juhasz, A. J.: Control of Exit Velocity Profile of an Asymmetric Annular Diffuser Using Wall Suction. NASA TM X-2710, 1972.

32. Anon.: Procedure for the Continuous Sampling and Measurement of Gaseous Emissions from Aircraft Turbine Engines. Aerospace Recommended Practice 1256, SAE, 1971.

33. Anon.: Aircraft Gas Turbine Exhaust Smoke Measurement. Aerospace Recommended Practice 1179, SAE, 1970.

34. Perkins, P. J.; Schultz, D. F.; and Wear, J. D.: Full-Scale Tests of a Short Length, Double-Annular Ram-Induction Turbojet Combustor for Supersonic Flight. NASA TN D-6254, 1971.

35. Clements, T. R.: 90-Degree Sector Development of a Short Length Combustor for a Supersonic Cruise Turbofan Engine. Rep. PWA-FR-3790, Pratt & Whitney Aircraft (NASA CR-72734), 1970.

36. Schultz, D. F.; and Perkins, P. J.: Effects of Radial and Circumferential Inlet Velocity Profile Distortions on Performance of a Short-Length Double-Annular Ram-Induction Combustor. NASA TN D-6706, 1972.

37. Schultz, D. F.; and Mularz, E. J.: Factors Affecting Altitude Relight Performance of a Double-Annular Ram-Induction Combustor. NASA TM X-2630, 1972.

38. Clements, T. R.: Development of a Short Length Combustor for a Supersonic Cruise Turbofan Engine Using a 90-Degree Sector of a Full Annulus. Rep. PWA-FR-4854, Pratt & Whitney Aircraft (NASA CR-120908), 1972.

39. Wear, J. D.; Perkins, P. J.; and Schultz, D. F.: Tests of a Full-Scale Annular Ram-Induction Combustor for a Mach 3 Cruise Turbojet Engine. NASA TN D-6041, 1970.

40. Rusnak, J. P.; and Shadowen, J. H.: Development of an Advanced Annular Combustor. Rep. PWA-FR-2832, Pratt & Whitney Aircraft (NASA CR-72453), 1969.

41. Pompei, Francesco; and Heywood, John B.: The Role of Mixing in Burner Generated Carbon Monoxide and Nitric Oxide. Rep. 722, Dept. Mech. Eng., Massachusetts Inst. of Tech., Feb. 1972.

42. Bahr, Donald W.: Technology for the Reduction of Aircraft Turbine Engines Exhaust Emissions. Atmospheric Pollution by Aircraft Engines, AGARD-CP-125, 1973, pp. 29-1 through 29-13.

43. Norgren, Carl T.; and Ingebo, Robert D.: Effect of Fuel Vapor Concentrations on Combustor Emissions and Performance. NASA TM X-2800, 1973.

44. Fletcher, Donald S.; and Heywood, John B.: A Model for Nitric Oxide Emissions from Aircraft Gas Turbine Engines. Paper 71-123, AIAA, Jan. 1971.

45. Heywood, J. B.: Gas Turbine Combustor Modelling for Calculating Nitric Oxide Emissions. Paper 71-712, AIAA, 1971.

46. Pompei, F.; and Heywood, J. B.: The Role of Mixing in Burner Generated Carbon Monoxide and Nitric Oxide. Comb. and Flame, vol. 19, no. 3, Dec. 1972, pp. 407-418.

47. Anderson, David N.: Effect of Premixing on Nitric Oxide Formation. NASA TM X-68220, 1973.

48. Edelman, Raymond; and Economos, Constantino: A Mathematical Model for Jet Engine Combustor Pollutant Emissions. Paper 71-714, AIAA, June 1971.

49. Weber, Richard J.; Dugan, James F., Jr.; and Luidens, Roger W.: Methane-Fueled Propulsion Systems. Paper 66-685, AIAA, June 1966.

50. Whitlow, John B., Jr.; Eisenberg, Joseph D.; and Shovlin, Michael D.: Potential of Liquid-Methane Fuel for Mach 3 Commercial Supersonic Transports. NASA TN D-3471, 1966.

51. Joslin, C. L.: The Potential of Methane as a Fuel for Advanced Aircraft. Aviation and Space: Progress and Prospects. (Proceedings of the Annual Aviation and Space Conference), 1968, pp. 351-355.

52. Esgar, Jack B.: Cryogenic Fuels for Aircraft. Aircraft Propulsion. NASA SP-259, 1970, pp. 397-420.

53. Schultz, Donald F.; Perkins, Porter J.; and Wear, Jerrold D.: Comparison of ASTM-A1 and Natural Gas Fuels in an Annular Turbojet Combustor. NASA TM X-52700, 1969.

54. Marchionna, Nicholas R.; and Trout, Arthur M.: Turbojet Combustor Performance with Natural Gas Fuel. NASA TN D-5571, 1970.

55. Fear, James S.; and Tacina, Robert R.: Performance of a Turbojet Combustor Using Natural Gas Fuel Heated to 1200° F (922 K). NASA TN D-5672, 1970.

56. Marchionna, Nicholas R.: Stability Limits and Efficiency of Swirl-Can Combustor Modules Burning Natural Gas Fuel. NASA TN D-5733, 1970.

57. Marchionna, Nicholas R.; and Trout, Arthur M.: Experimental Performance of a Modular Turbojet Combustor Burning Natural Gas Fuel. NASA TN D-7020, 1970.

58. Trout, Arthur M.; and Marchionna, Nicholas R.: Effect of Inlet Air Vitiation on the Performance of a Modular Combustor Burning Natural Gas Fuel. NASA TM X-52711, 1969.

59. Humenik, Francis M.: Conversion of an Experimental Turbojet Combustor from ASTM A-1 Fuel to Natural Gas Fuel. NASA TM X-2241, 1971.

60. Wear, Jerrold D.; and Schultz, Donald F.: Effects of Fuel Nozzle Design on Performance of an Experimental Annular Combustor Using Natural Gas Fuel. NASA TN D-7072, 1972.

61. Hibbard, R. R.: Evaluation of Liquified Hydrocarbon Gases as Turbojet Fuels. NACA RM E56I2I, 1956.

62. Wear, J. D.; and Jones, R. E.: Comparison of the Combustion Characteristics of ASTM A1, Propane, and Natural Gas Fuels in an Advanced Annular Combustor. NASA TN D-7135, 1972.

63. Hilt, M. B.; and Johnson, R. H.: Nitric Oxide Abatement in Heavy Duty Gas Turbine Combustors by Means of Aerodynamics and Water Injection. Paper 72-GT-53, ASME, Mar. 1972.

64. Grobman, Jack; and Norgren, Carl; and Anderson, David: Turbojet Emissions, Hydrogen Versus JP. NASA TM X-68258, 1973.

65. Silverstein, Abe; and Hall, Eldon W.: Liquid Hydrogen as a Jet Fuel for High-Altitude Aircraft. NACA RM E55C28a, 1955.

66. Lewis Laboratory Staff: Hydrogen for Turbojet and Ramjet Powered Flight. NACA RM E57D23, 1957.

67. Kaufman, Harold R.: High-Altitude Performance Investigation of J65-B-3 Turbojet Engine with both JP-4 and Gaseous Hydrogen Fuels. NACA RM E57A11, 1957.

68. Friedman, Robert; Norgren, Carl T.; and Jones, Robert E.: Performance of a Short Turbojet Combustor with Hydrogen Fuel in a Quarter-Annulus Duct and Comparison with Performance in a Full-Scale Engine. NACA RM E56D16, 1956.

69. Rayle, Warren D.; Jones, Robert E.; and Friedman, Robert: Experimental Evaluation of "Swirl-Can" Elements for Hydrogen-Fuel Combustor. NACA RM E57C18, 1957.

70. Jones, Robert E.; and Rayle, Warren D.: Performance of Five Short Multielement Turbojet Combustors for Hydrogen Fuel in Quarter-Annulus Duct. NACA RM E58D15, 1958.

71. Smith, Arthur L.; and Grobman, Jack: Exploratory Investigation of Performance of Experimental Fuel-Rich Hydrogen Combustion System. NACA RM E58C19a, 1958.

72. Drell, Isadore L.; and Belles, Frank E.: Survey of Hydrogen Combustion Properties. NACA Rep. 1383, 1958.

73. Barnett, H. C.; and Hibbard, R. R., eds.: Basic Considerations in the Combustion of Hydrocarbon Fuels with Air. NACA Rep. 1300, 1957.

74. Longwell, John P.; and Weiss, Malcolm A.: High Temperature Reaction Rates in Hydrocarbon Combustion. Ind. & Eng. Chem. vol. 47, no. 8, Aug. 1955, pp. 1634-1643.

75. Norgren, Carl T.; and Ingebo, Robert D.: Emissions of Nitrogen Oxides From An Experimental Hydrogen-Fueled Gas Turbine Combustor. TM X-2997, 1974.

76. Cervenka, A. J.; and Friedman, R.: Ram-Jet Performance. Adaptation of Combustion Principles to Aircraft Propulsion. Vol. II - Combustion in Air-Breathing Jet Engines. NACA RM E55G28, 1956, Ch. XIV.

77. Alexander, Arthur D., III: Economic Study of Future Aircraft Fuels (1970-2000). NASA TM X-62180, 1972.

78. Kraft, Gerald A.: Optimization of Engines for a Commercial Mach 0.85 Transport Using Advanced Turbine Cooling Methods. NASA TM X-68173, 1972.

79. Whitlow, John B., Jr.; Weber, Richard J.; and Civinskas, Kestutis C.: Preliminary Appraisal of Hydrogen and Methane in a Mach 2.7 Supersonic Transport. NASA TM X-68222, 1973.

80. Anon.: Environmental Protection Agency Control of Air Pollution from Aircraft and Aircraft Engines Emission Standards and Test Procedures for Aircraft. Federal Register, vol. 38, no. 136, pt. 2, July 17, 1973, pp. 19088-19103.

81. Gordon, Sanford; and McBride, Bonnie J.: Computer Program for Calculation of Complex Chemical Equilibrium Compositions, Rocket Performance, Incident and Reflected Shocks, and Chapman-Jouquet Detonations. NASA SP-273, 1971.

82. Bittker, David A.; and Scullin, Vincent J.: General Chemical Kinetics Computer Program for Static and Flow Reactions, with Application to Combustion and Shock Tube Kinetics. NASA TN D-6586, 1972.

83. Boccio, J. L.; Weilerstein, G.; and Edelman, R. B.: A Mathematical Model for Jet Engine Combustor Pollutant Emissions. GASL-TR-781, General Applied Science Labs., Inc. (NASA CR-121208), 1973.

84. Homer, J. B.; and Sutton, M. M.: Nitric Oxide Formation and Radical Overshoot in Premixed Hydrogen Flames. Comb. and Flame, vol. 20, no. 1, Feb. 1973, pp. 71-76.

85. Marchionna, Nicholas R.; Diehl, Larry A.; and Trout, Arthur M.: Effect of Inlet-Air Humidity, Temperature, Pressure, and Reference Mach Number on the Formation of Oxides of Nitrogen in a Gas Turbine Combustor. NASA TN D-7396, Oct. 1973.

86. Broderick, A. J.; English, J. M.; and Forney, A. K.: An Initial Estimate of Aircraft Emissions in the Stratosphere in 1990. Paper 73-508, AIAA, June 1973.

TABLE I. - CONSTITUENTS OF JET AIRCRAFT ENGINE EXHAUST

AT TYPICAL TAKEOFF AND CRUISE CONDITIONS

Constituent	Source	Estimated concentration[a]
N_2	Air	77 vol. %
O_2	Air	16.6 vol. %
A	Air	0.9 vol. %
H_2O	Complete combustion	2.7 vol. %
CO_2	Complete combustion	2.8 vol. %
CO	Incomplete combustion	10 to 50 ppm[a]
Unburned and partially oxidized hydrocarbons	↓	5 to 25 ppm[a]
H_2	↓	5 to 50 ppm[a]
Smoke (particulates)	↓	0.4 to 50 ppm[b]
NO, NO_2	Heating of air	50 to 400 ppm[a]
SO_2, SO_3	Fuel	1 to 10 ppm[a]
Trace metals	Fuel	5 to 20 ppm[b]

[a]By volume.

[b]By mass.

TABLE II. - CAUSES AND TYPICAL LEVELS OF JET AIRCRAFT EMISSIONS

Pollutant	Critical operating condition	Typical emission level	Major causes
Hydrocarbons	Idle	7 to 75 g/kg fuel	Poor fuel atomization Lean fuel-air ratios
Carbon monoxide	Idle	30 to 77 g/kg fuel	Low combustor pressure and temperature
Oxides of nitrogen	Takeoff Cruise	13 to 40 g/kg fuel 10 to 20 g/kg fuel	High flame temperature

TABLE III. - CHARACTERISTICS OF COMMERCIAL AIRCRAFT SYSTEMS

(a) Subsonic

Characteristic	Production turbofans (CTOL)		Future turbofans (ATT)		
Fuel	JP	JP	JP	LNG	Hydrogen
Aircraft designation	747B-200	DC-10 (series 30)	----------	----------	----------
Takeoff gross weight, kg	354 000	252 000	113 000	102 000	68 000
Number of passengers	374 to 500	250 to 380	200	200	200
Range, km	11 900	9550	5560	5560	5560
Cruise Mach number	0.85	0.85	0.85	0.85	0.85
Cruise altitude, m	10 700	10 700	12 200	12 200	12 200
Engine make and model	P&WA JT9D-7	GE CF6-50	----------	----------	----------
Number of engines	4	3	3	3	3
Noise level, EPNdB	107	105	96	96	96
Maximum power at sea level, N (lbf)	209 000 (47 000)	227 000 (51 000)	115 000 (25 800)	104 000 (23 400)	69 400 (15 600)
Specific fuel consumption at maximum power, kg-hr/N (lbm-hr/lbf	0.037 (0.36)	0.040 (0.39)	0.056 (0.55)	0.048 (0.474)	0.020 (0.198)
Overall compression ratio at maximum power	23	29.4	23.9	23.9	23.9
Maximum power at cruise, N (lbf)	----------	----------	18 260 (4100)	16 460 (3700)	10 990 (2470)
Specific fuel consumption at cruise, kg-hr/N (lbm-hr/lbf)	----------	----------	0.073 (0.718)	0.063 (0.619)	0.026 (0.258)
Overall compression ratio at cruise	----------	----------	26.4	26.4	26.4

(b) Supersonic

Characteristic	Concorde afterburning turbojet	Future duct-burning turbofans (ASST)		
Fuel	JP	JP	LNG	Hydrogen
Takeoff gross weight, kg	175 000	382 000	348 000	229 000
Number of passengers	128	250	250	250
Range, km	5900	7400	7400	7400
Cruise Mach number	2.0	2.7	2.7	2.7
Cruise altitude, m	17 700	19 800	19 800	19 800
Engine model	Olympus 593	----------	----------	----------
Number of engines	4	4	4	4
Noise level, EPNdB	115	108	108	108
Maximum power at sea level, N (lbf)	170 000 (38 050)	306 000 (68 700)	278 000 (62 400)	183 000 (41 100)
Specific fuel consumption at maximum power, kg-hr/N (lbm-hr/lbf)	----------	0.078 (0.763)	0.067 (0.657)	0.028 (0.2745)
Overall compression ratio at maximum power	14.8	10	10	10
Maximum power at cruise, N (lbf)	29 650 (6666)	85 600 (19 250)	75 840 (17 050)	68 940 (15 500)
Specific fuel consumption at cruise, kg-hr/N (lbm-hr/lbf)	0.121 (1.189)	0.157 (1.54)	0.135 (1.32)	0.057 (0.56)
Overall compression ratio at cruise	----------	4	4	4

TABLE IV. - CRUISE OPERATING CONDITIONS

(a) Subsonic

Condition	Production turbofan (P&WA JT9D-7)	Future turbofans (ATT)		
Fuel	JP	JP	LNG	Hydrogen
Cruise Mach number	0.85	0.85	0.85	0.85
Cruise altitude, m	10 700	12 200	12 200	12 200
Total airflow rate, kg/sec	304	151	136	90.6
Bypass ratio	4.9	7.8	7.8	7.8
Compressor discharge airflow rate, kg/sec	51.5	17.2	15.5	10.3
Combustor inlet temperature, K	710	661	661	661
Combustor inlet pressure, atm	9.7	7.2	7.2	7.2
Combustor exit temperature, K	1410	1540	1540	1540
Fuel-air ratio	0.018	0.026	0.023	0.0096
Fuel flow rate (per engine), kg/hr	2800	1610	1280	356

(b) Supersonic

Condition	Concorde afterburning turbojet (Olympus 593)[a]	Future duct-burning turbofans (ASST)		
Fuel	JP	JP	LNG	Hydrogen
Cruise Mach number	2.0	2.7	2.7	2.7
Cruise altitude, m	17 700	19 800	19 800	19 800
Total airflow rate, kg/sec	83	336	306	202
Bypass ratio	0	2.36	2.36	2.36
Compressor discharge airflow rate, kg/sec	83	100	91	61
Combustor inlet total temperature, T_3, K	824	810	810	810
Combustor inlet total pressure, P_3, atm	6.5	4.7	4.7	4.7
Combustor exit average temperature, K	1320	1770	1770	1770
Combustor fuel-air ratio	0.0141	0.0299	0.0265	0.01187
Combustor fuel flow rate, kg/hr	4200	10 750	8700	2560
Augmentor airflow rate, kg/sec	------	236	215	141
Augmentor inlet total temperature, K	------	635	635	635
Augmentor inlet total pressure, atm	------	2.6	2.6	2.6
Augmentor inlet velocity, m/sec	------	90	90	90
Augmentor exit average temperature, K	------	835	835	835
Augmentor fuel-air ratio	------	0.00495	0.0045	0.00187
Augmentor fuel flow rate, kg/hr	------	4200	3500	940
Total fuel flow rate (per engine), kg/hr	4200	14 950	12 200	3500

[a]Afterburner is not used for steady-state cruise.

TABLE V. - CLASSES OF PROJECTED COMBUSTION SYSTEM DESIGN

MODIFICATIONS TO REDUCE EMISSIONS DURING CRUISE

Class	Modification	Descriptive examples
1	Minor modification: Retrofit production engine Minor change or improvement to growth version of production engine	Substitute improved fuel injector to improve fuel atomization
2	Major modification - advanced state of the art	Utilize Experimental Clean Combustor Program technology

TABLE VI. - PROJECTED COMBUSTOR TECHNOLOGY

(a) Subsonic (CTOL) aircraft

Engine	Fuel	Class of modification	Description
Retrofit production turbofan or advanced turbofan	JP	1	Substitution of improved air-atomizing fuel injectors in a conventional combustion liner
Advanced turbofan	JP	2	Use of Experimental Clean Combustor Program technology, such as swirl-can combustor
	LNG	1	Incorporation of vapor injection in a conventional combustion liner
	LNG	2	Use of LNG swirl-can combustor
	Hydrogen	1	Incorporation of vapor injectors in a conventional combustion liner
	Hydrogen	2	Use of hydrogen swirl-can combustor

(b) Supersonic aircraft

Retrofit production afterburning turbojet	JP	1	Substitution of improved air-atomizing fuel injectors in conventional combustor No major changes to afterburner
Duct-burning turbofan	JP	1	Substitution of improved air-atomizing fuel injectors in conventional combustor Use of ram-induction duct burner (ref. 7)
	JP	2	Use of Experimental Clean Combustor Program technology, such as swirl-can combustor Use of advanced duct burner
	LNG	1	Incorporation of vapor injectors in a conventional combustor Use of ram-induction duct burner (ref. 7)
	LNG	2	Use of LNG swirl-can combustor Use of advanced duct burner
	Hydrogen	1	Incorporation of vapor injectors in a conventional combustor Use of ram-induction duct burner (ref. 7)
	Hydrogen	2	Use of hydrogen swirl-can combustor Use of advanced duct burner

TABLE VII. - ESTIMATED EMISSION INDICES AND EMISSION RATES AT CRUISE CONDITIONS

Constituent	JP	LNG	Hydrogen	Future turbofans (ATT)			Future duct-burning turbofans (ASST)		
	Emission index, g/kg fuel			JP	LNG	Hydrogen	JP	LNG	Hydrogen
				Emission rate (per engine), kg/hr					
H_2O	1.25×10^3	2.25×10^3	8.9×10^3	2000	2900	3200	18 700	27 500	31 200
CO_2	3.22×10^3	2.74×10^3	-------	5200	3500	----	48 100	33 400	------
Soot (as carbon)	0.1	--------	-------	0.2	----	----	1.5	------	------
SO_2	1 to 2	--------	-------	2 to 3	----	----	15 to 30	------	------
Total trace elements	0.01	--------	-------	0.02	----	----	0.15	------	------
Lubricating oil	0.1	0.1	0.1	0.2	0.1	0.04	1.5	1.2	0.4

TABLE VIII. - EXHAUST EMISSION ESTIMATES

FOR PRODUCTION PROPULSION SYSTEMS

AT CRUISE CONDITIONS

Pollutant	JT9D[a]	Olympus 593[b]
Oxides of nitrogen:		
g NO_2/kg fuel	16 to 23	18 to 19
kg NO_2/hr	45 to 64	76 to 80
Carbon monoxide:		
g CO/kg fuel	0.2 to 0.8	1 to 5
kg CO/hr	0.6 to 2	4 to 21
Total hydrocarbons:		
g CH_2/kg fuel	0.1 to 0.3	<1
kg CH_2/hr	0.3 to 0.8	<4
Combustion efficiency, percent	~100	99.9

[a]Based on ref. 5 (p. IV-311).

[b]Based on ref. 1 (pp. 173-179).

TABLE IX. - EXHAUST EMISSION PROJECTIONS FOR FUTURE PROPULSION SYSTEMS AT CRUISE CONDITIONS

(a) JP fuel

	Future turbofan (ATT)			Future duct-burning turbofan (ASST)								
				Core engine emissions			Augmentor emissions			Overall engine emissions		
	Class 1[a]	Class 2[b]	Minimum[c]	Class 1	Class 2	Minimum	Class 1	Class 2	Minimum	Class 1	Class 2	Minimum
Oxides of nitrogen:												
g NO_2/kg fuel	9 to 13	4 to 6	0.2 to 2	13 to 15	5 to 9	0.7 to 7	3	1	0.1 to 0.7	10 to 11	3 to 7	[d]0.7 to 7
kg NO_2/hr	14 to 21	6 to 10	0.3 to 3	140 to 160	50 to 100	10 to 100	13	4	0.3 to 3	150 to 170	50 to 100	10 to 100
Carbon monoxide:												
g CO/kg fuel	0.2 to 0.8	0.2 to 0.8	0.2 to 0.8	0.2 to 0.8	0.2 to 0.8	0.2 to 0.8	60	30	0.2 to 0.8	17.4	8.7	0.2 to 0.8
kg CO/hr	0.3 to 1	0.3 to 1	0.3 to 1	2 to 9	2 to 9	2 to 9	250	125	0.8 to 3	260	130	3 to 12
Total hydrocarbons:												
g CH_2/kg fuel	0.1 to 0.3	0.1 to 0.3	0.1 to 0.3	0.1 to 0.3	0.1 to 0.3	0.1 to 0.3	5	2.5	0.1 to 0.3	1.5	0.9	0.1 to 0.3
kg CH_2/hr	0.2 to 0.5	0.2 to 0.5	0.2 to 0.5	1 to 3	1 to 3	1 to 3	21	11	0.4 to 1	23	13	1 to 4
Combustion efficiency, percent	~100	~100	~100	~100	~100	~100	98	99	~100	---	---	---

(b) LNG fuel

Oxides of nitrogen:												
g NO_2/kg fuel	9 to 14	3.8	0.1 to 0.9	16 to 17	6	0.5 to 5	3	1	0.1 to 0.4	9 to 10	4	0.3 to 3
kg NO_2/hr	12 to 18	5	0.1 to 1	140 to 150	50	4 to 40	11	3.5	0.1 to 1	150 to 160	54	4 to 40
Carbon monoxide:												
g CO/kg fuel	0.2 to 0.8	0.2 to 0.8	0.2 to 0.8	0.2 to 0.8	0.2 to 0.8	0.2 to 0.8	60	30	0.2 to 0.8	17 to 18	9	0.2 to 0.8
kg CO/hr	0.3 to 1	0.3 to 1	0.3 to 1	2 to 7	2 to 7	2 to 7	210	105	0.7 to 3	210 to 220	110	3 to 10
Total hydrocarbons:												
g CH_2/kg fuel	0.1 to 0.3	0.1 to 0.3	0.1 to 0.3	0.1 to 0.3	0.1 to 0.3	0.1 to 0.3	5	2.5	0.1 to 0.3	1.6 to 1.7	0.8 to 1.9	0.1 to 0.3
kg CH_2/hr	0.1 to 0.4	0.1 to 4	0.1 to 0.4	1 to 3	1 to 3	1 to 3	18	9	0.4 to 1	19 to 21	10 to 12	1 to 4
Combustion efficiency, percent	~100	~100	~100	~100	~100	~100	98	99	~100	---	---	---

(c) Hydrogen fuel

Oxides of nitrogen:												
g NO_2/kg fuel	38 to 54	11	<0.1	53 to 58	17	0.1 to 1	8	3	≤0.1	43 to 46	14	0.1 to 1
kg NO_2/hr	14 to 20	4	<0.04	140 to 150	44	0.3 to 3	7.5	3	≤0.1	150 to 160	50	0.3 to 3

[a]Minor combustor modification.

[b]Major combustor modification.

[c]Minimum theoretical limit from chemical kinetics calculations.

[d]Upper and lower limits represent minimum primary-zone equivalence ratios of 0.6 and 0.5, respectively.

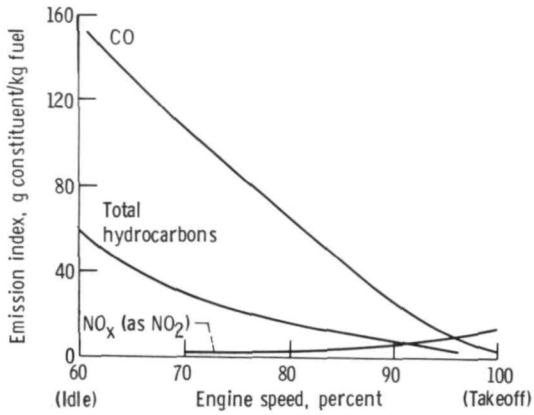

Figure 1. - Typical engine emission characteristics. Engine pressure ratio, 13.4; fuel, JP-5.

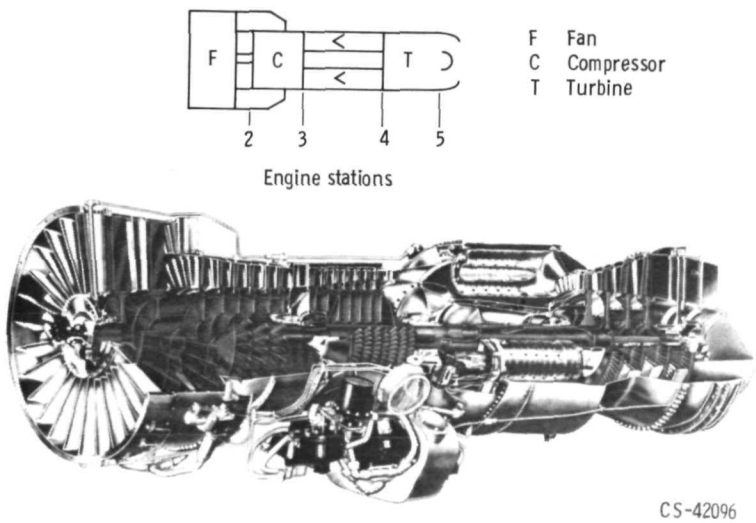

Figure 2. - Turbofan engine.

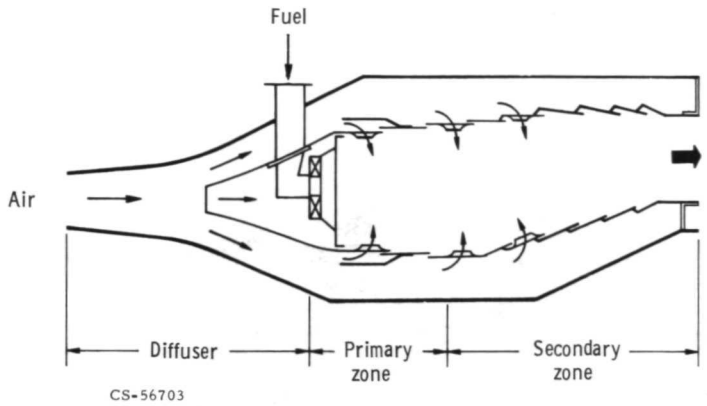

Figure 3. - Conventional annular combustor.

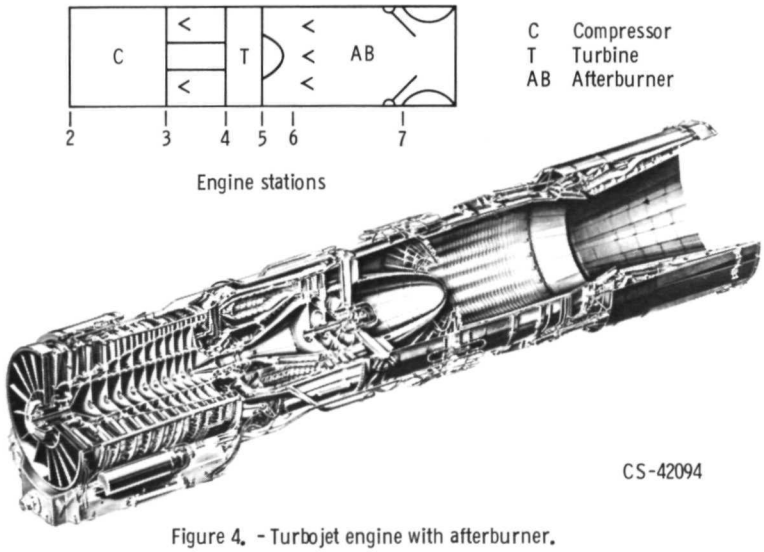

Figure 4. - Turbojet engine with afterburner.

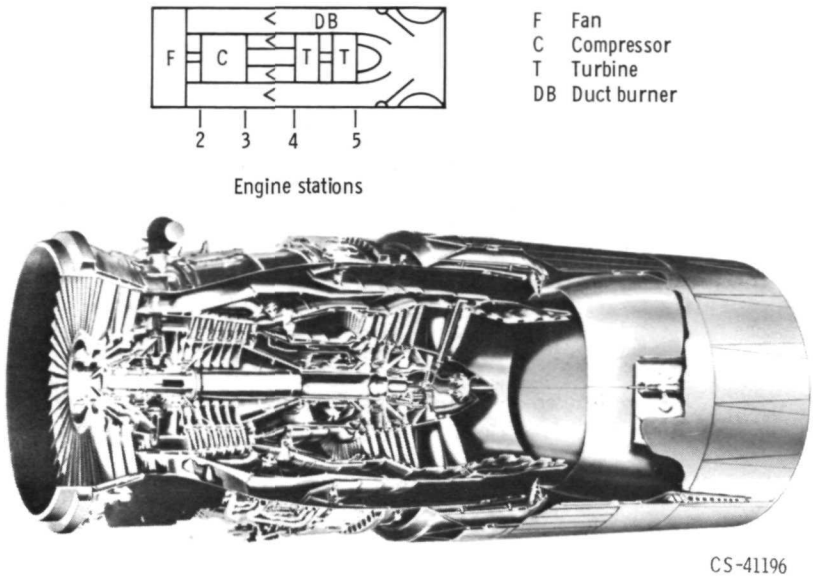

Figure 5. - Duct-burning turbofan.

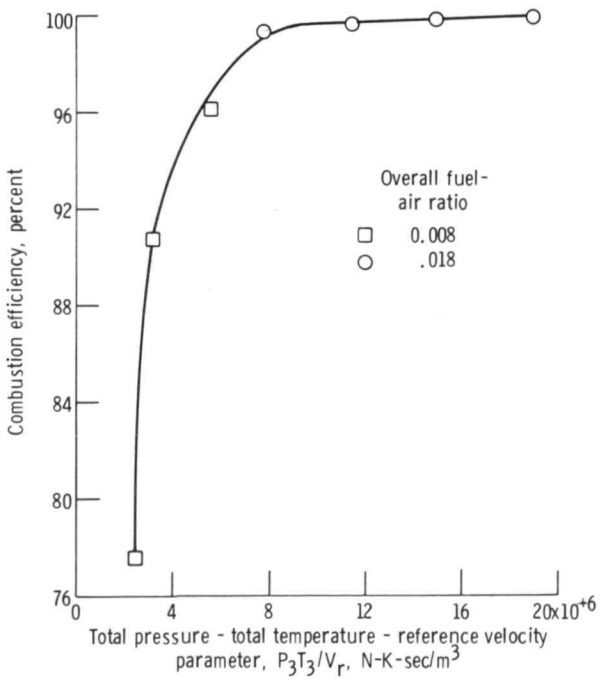

Figure 6. - Correlation of PT/V parameter with combustion efficiency.

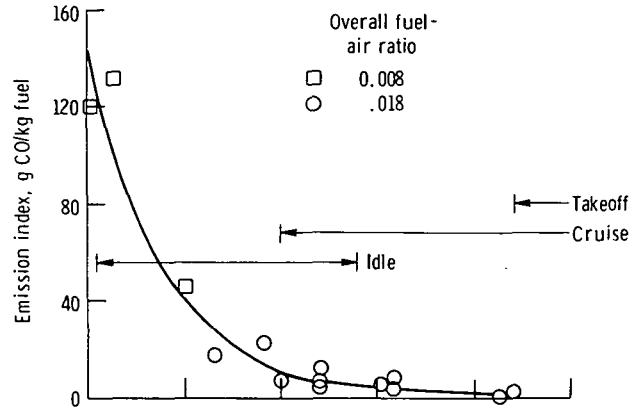

(a) Carbon monoxide emissions.

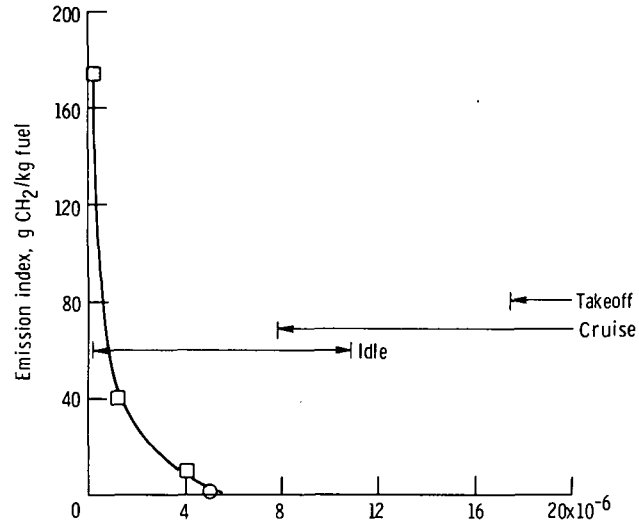

(b) Total hydrocarbon emissions.

Figure 7. - Correlation of PT/V parameter with carbon monoxide and total hydrocarbon emission indices.

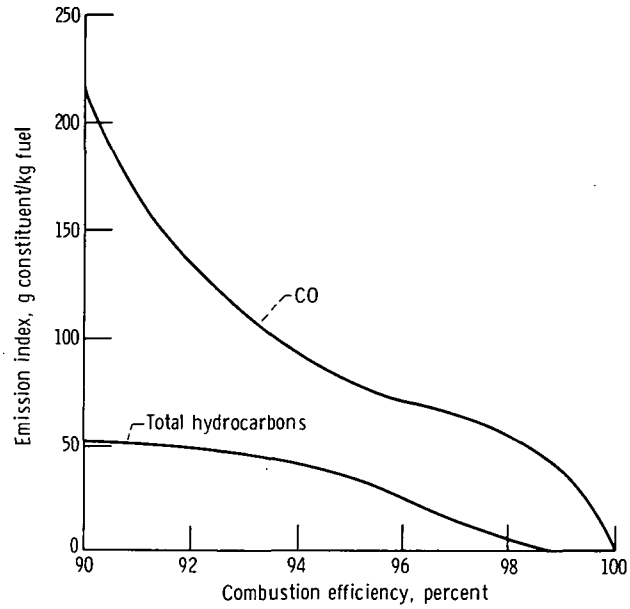

Figure 8. - Variation of levels of carbon monoxide and total hydrocarbons with combustion efficiency.

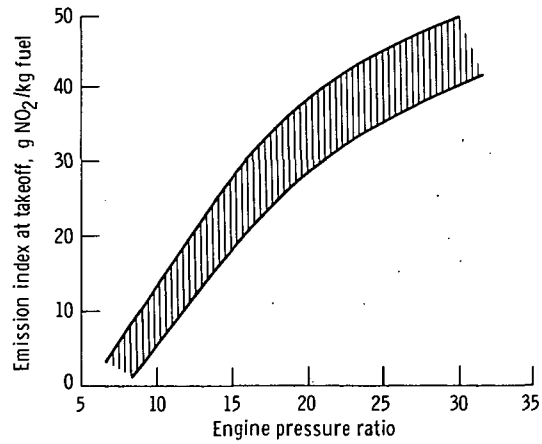

Figure 9. - Variation of oxides-of-nitrogen emission index with engine pressure ratio.

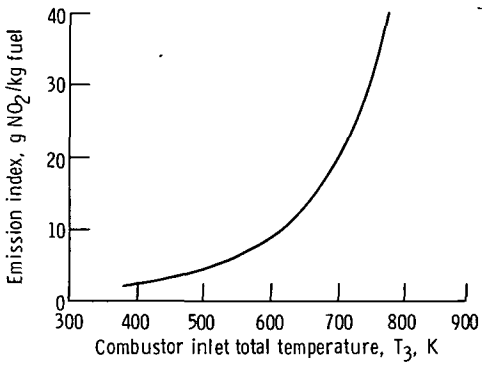

Figure 10. - Variation of oxides-of-nitrogen emission index with combustor inlet total temperature for production engines.

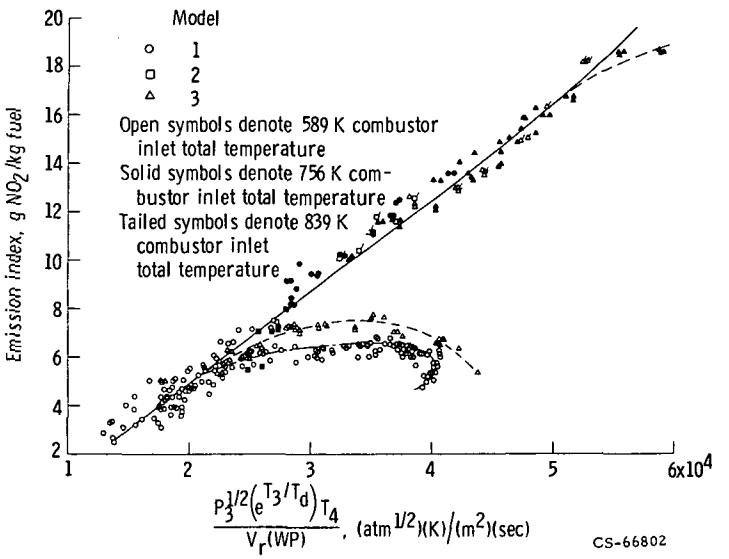

Figure 11. - Correlation of operating variables with oxides-of-nitrogen emission index for a swirl-can combustor.

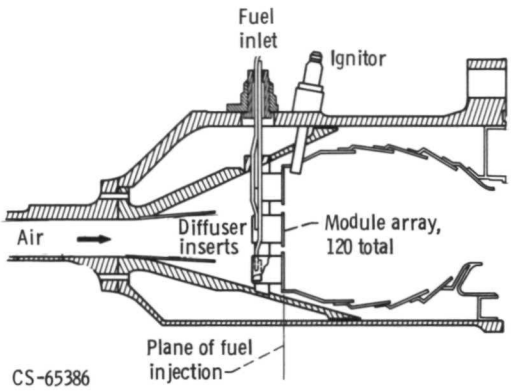

Figure 12. - Full-annular model of a swirl-can combustor.

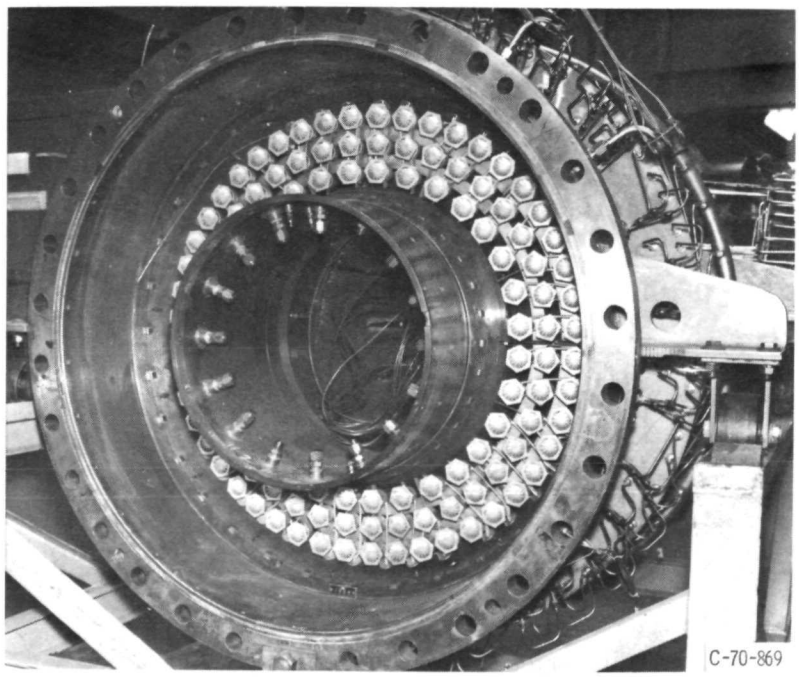

Figure 13. - Annular swirl-can modular combustor.

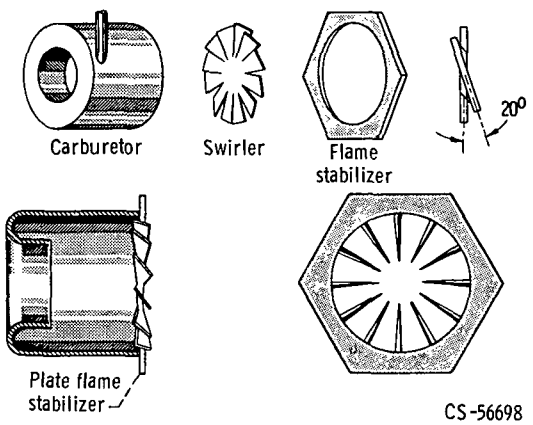

Figure 14. - Details of swirl-can combustor module.

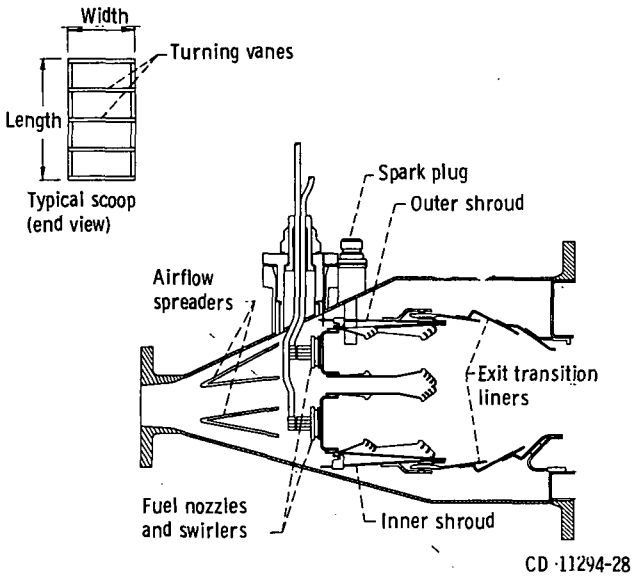

Figure 15. - Cross section of double-annular ram-induction combustor. (Dimensions are in centimeters.)

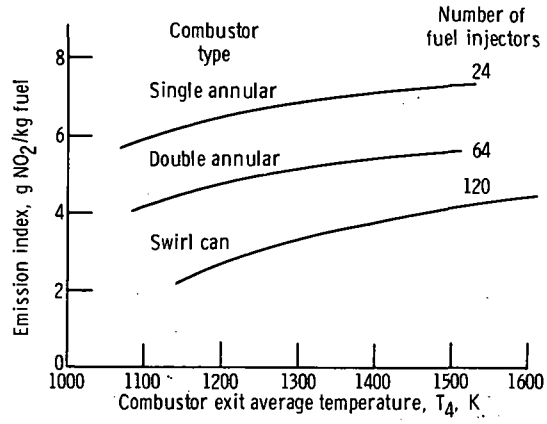

Figure 16. - Variation of oxides-of-nitrogen emission index with combustor exit average temperature for single-zone and multizone combustors. Combustor inlet total temperature, T_3, 590 K; combustor inlet total pressure, P_3, 6 atmospheres; reference velocity, V_r, 32 m/sec.

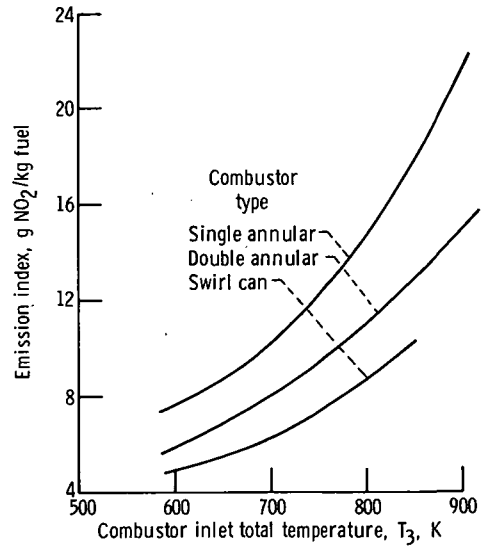

Figure 17. - Variation of oxides-of-nitrogen emission index with combustor inlet total temperature for single-zone and multizone combustors. Combustor inlet total pressure, P_3, 6 atmospheres; combustor exit average temperature, T_4, 1500 K.

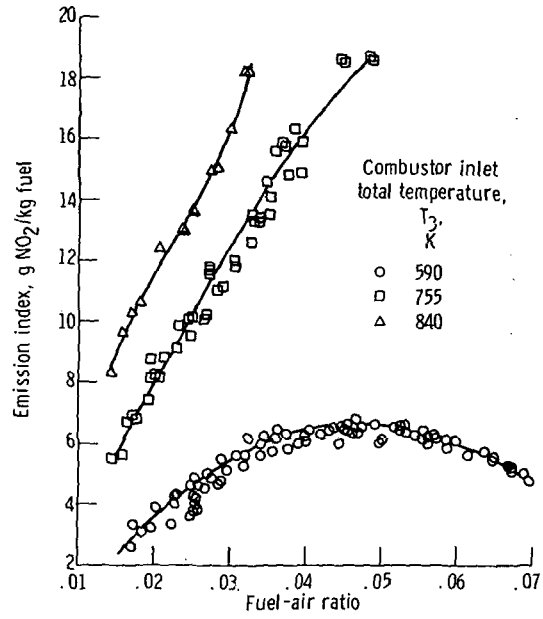

Figure 18. - Variation of oxides-of-nitrogen emission index with combustor inlet total temperature and fuel-air ratio for a swirl-can combustor. Combustor inlet total pressure, P_3, 5 to 6 atmospheres; airflow, 38.5 to 50 kg/sec.

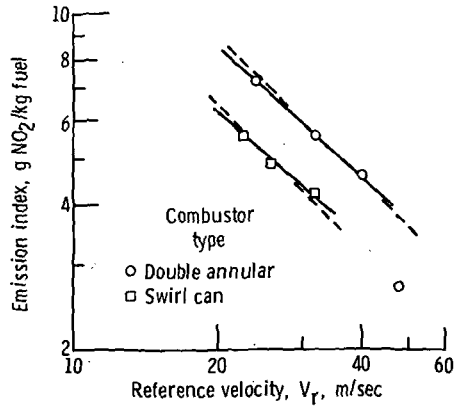

Figure 19. - Variation of oxides-of-nitrogen emission index with reference velocity for multizone combustors. Combustor inlet total temperature, T_3, 590 K; combustor inlet total pressure, P_3, 6 atmospheres.

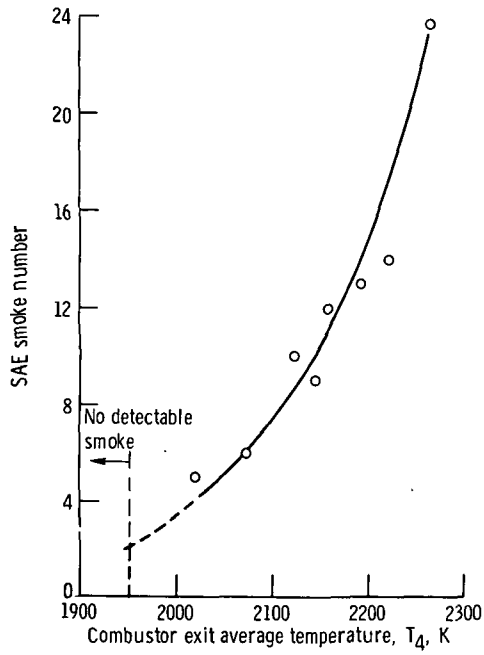

Figure 20. - Variation of smoke number with combustor exit average temperature for a swirl-can combustor. Combustor inlet total temperature, T_3, 590 K; combustor inlet total pressure, P_3, 6 atmospheres.

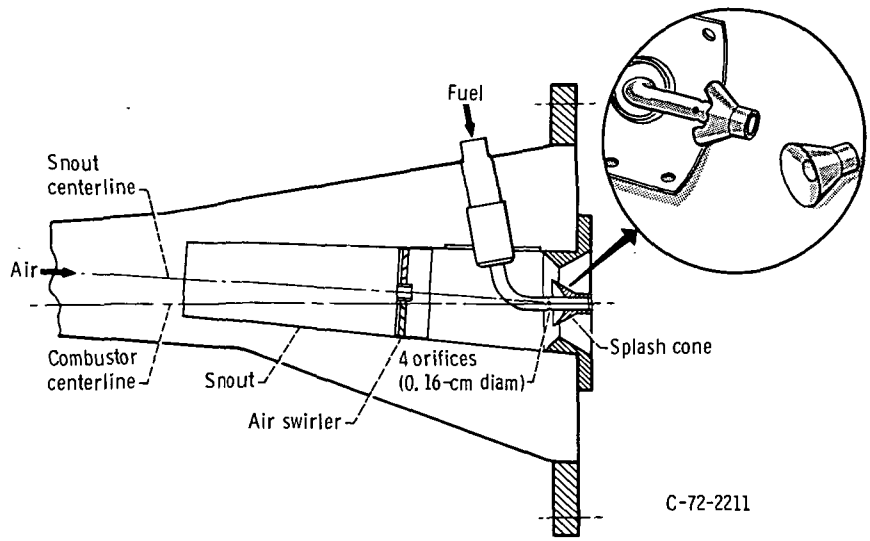

Figure 21. - Air-atomizing splash-cone fuel injectors.

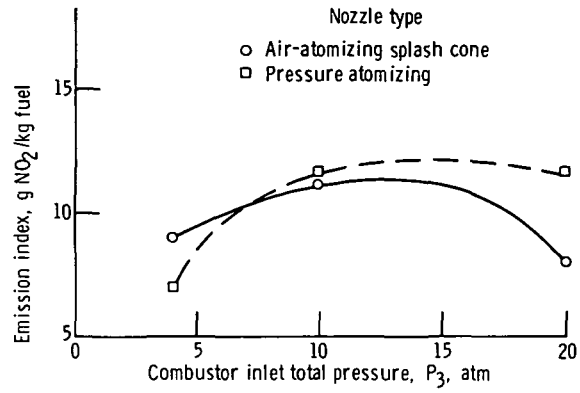

Figure 22. - Variation of oxides-of-nitrogen emission index with combustor inlet total pressure for air- and pressure-atomizing fuel injectors. Combustor inlet total temperature, T_3, 590 K; fuel-air ratio, 0.015.

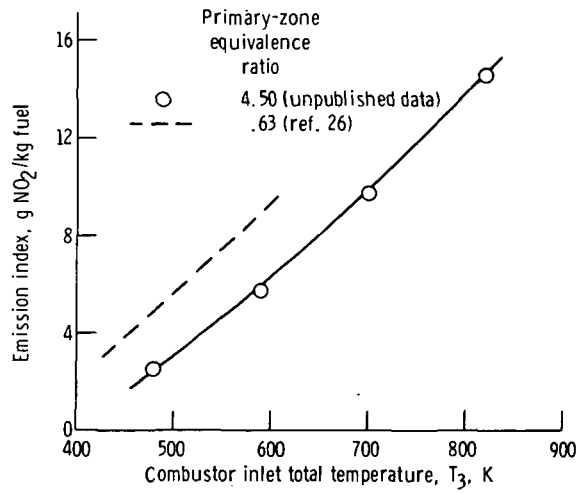

Figure 23. - Variation of oxides-of-nitrogen emission index with combustor inlet total temperature for air-atomizing splash-cone fuel injectors. Combustor inlet total pressure, P_3, 4 atmospheres; fuel-air ratio, 0.015.

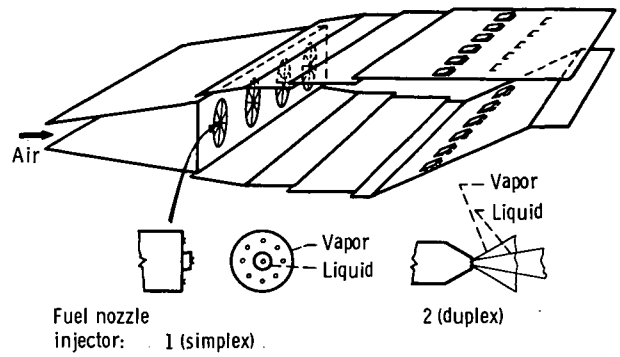

Figure 24. - Test combustor with dual fuel-injection system for liquid Jet A and gaseous propane.

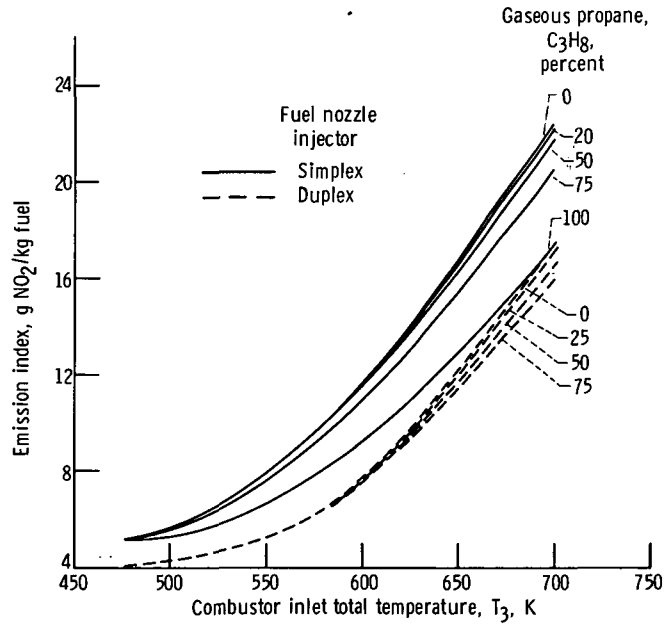

Figure 25. - Variation in oxides-of-nitrogen emission index with combustor inlet total temperature for various percentages of gaseous propane. Combustor inlet total pressure, P_3, 10 atmospheres; fuel-air ratio, 0.014; reference velocity, V_r, 21.3 m/sec.

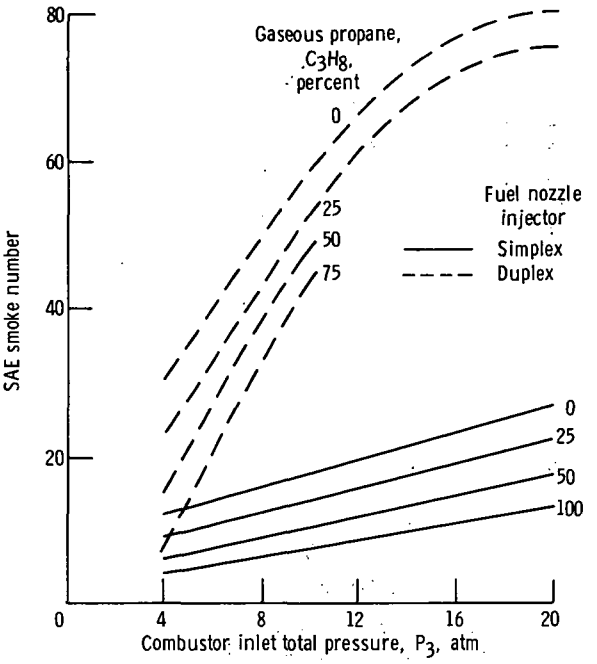

Figure 26. - Variation in smoke number with combustor inlet total pressure for various percentages of gaseous propane. Combustor inlet total temperature, T_3, 590 K; fuel-air ratio, 0.010.

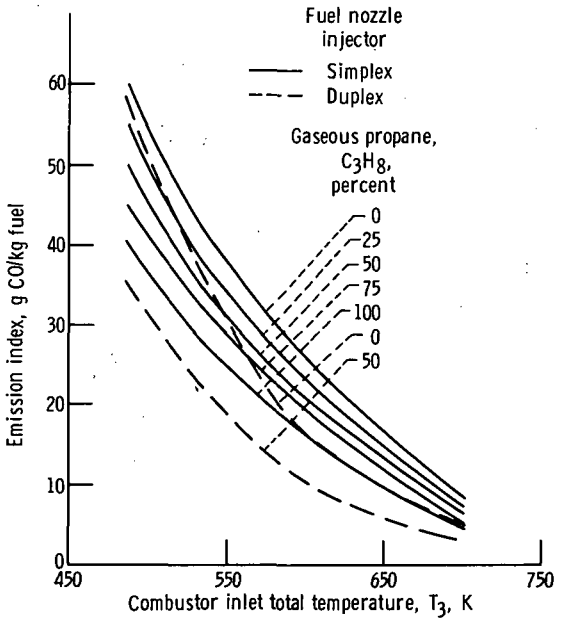

Figure 27. - Variation in carbon monoxide emission index with combustor inlet total temperature for various percentages of gaseous propane. Combustor inlet total pressure, P_3, 10 atmospheres; fuel-air ratio, 0.014.

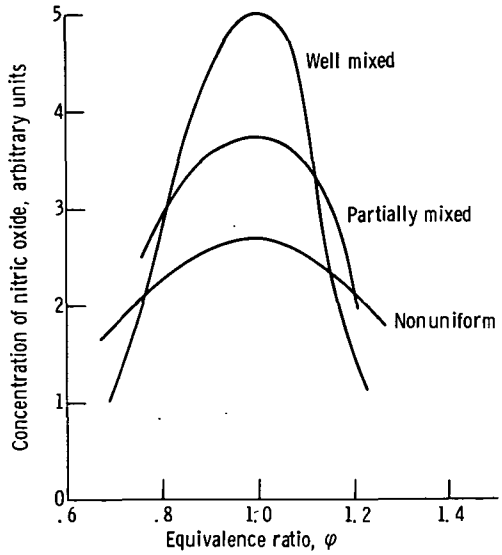

Figure 28. - Variation of nitric oxide concentration with equivalence ratio distribution (crossplot of analytical results presented in fig. 4 of ref. 44).

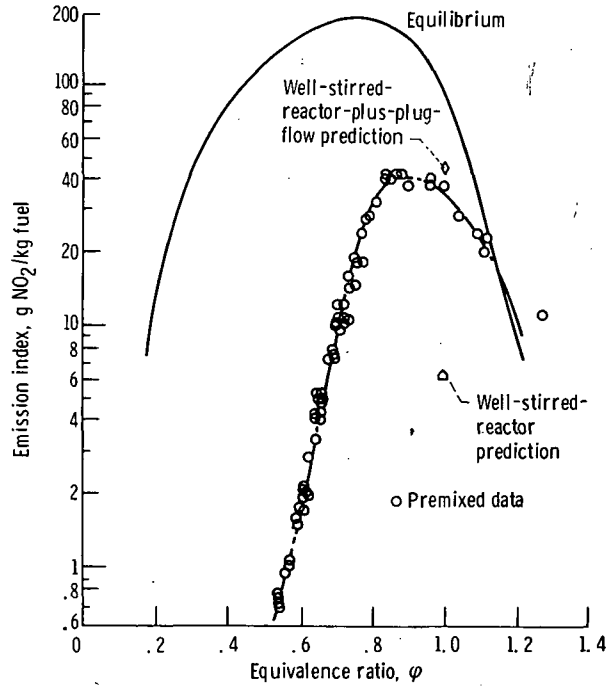

Figure 29. - Variation of oxides-of-nitrogen emission index with equivalence ratio distribution for a flame-tube burning premixed gaseous propane. Combustor inlet total temperature, T_3, 590 K; combustor inlet total pressure, P_3, 5.5 atmospheres; reference velocity, V_r, 23 m/sec.

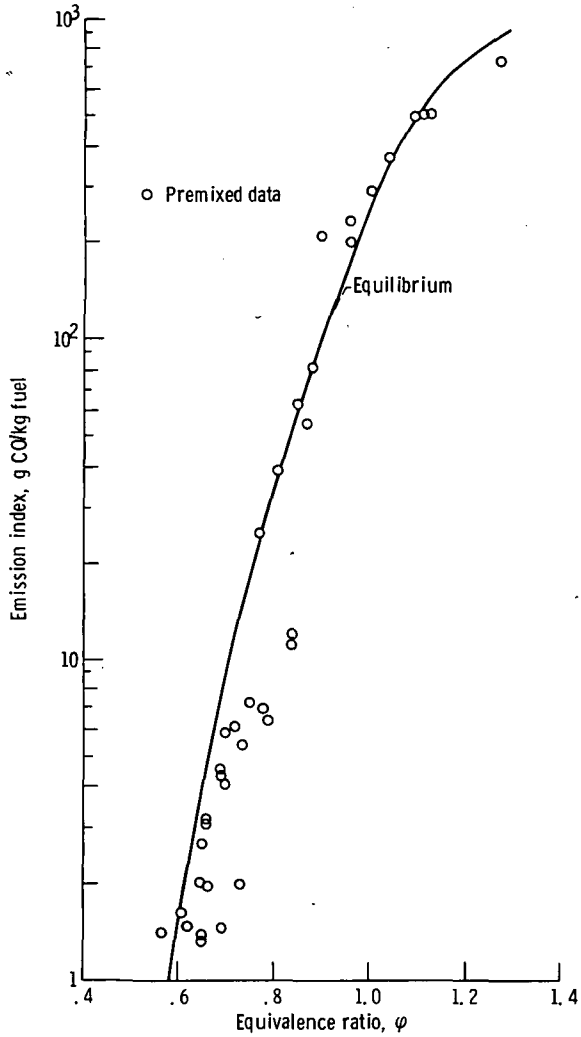

Figure 30. - Variation of carbon monoxide emission index with equivalence ratio for a flame-tube burning premixed gaseous propane. Combustor inlet total temperature, T_3, 590 K; combustor inlet total pressure, P_3, 5.5 atmospheres; reference velocity, V_r, 23 m/sec.

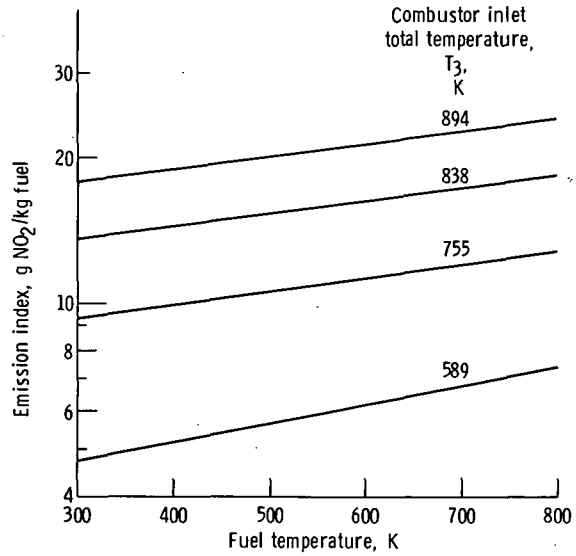

Figure 31. - Variation of oxides-of-nitrogen emission index with fuel temperature for liquefied natural gas. Combustor inlet total pressure, P_3, 6 atmospheres; reference Mach number, 0.065.

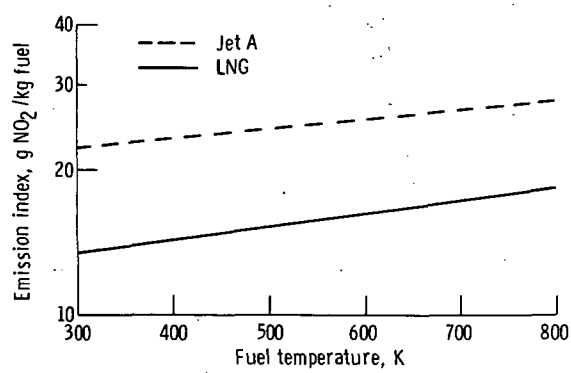

Figure 32. - Variation of oxides-of-nitrogen emission index with fuel temperature for liquefied natural gas and Jet A at typical aircraft cruise conditions: combustor inlet total temperature, T_3, 840 K; combustor inlet total pressure, P_3, 6 atmospheres; reference Mach number, 0.065.

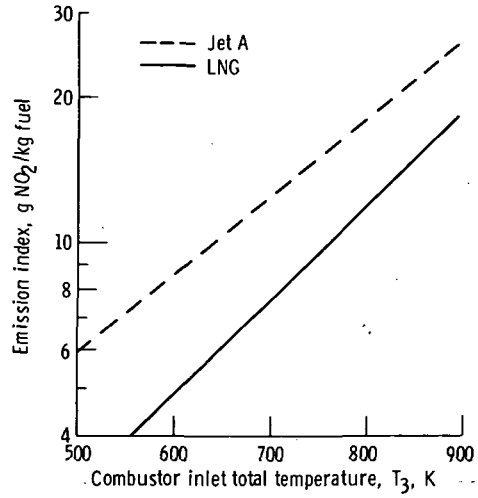

Figure 33. - Variation of oxides-of-nitrogen emission index with combustor inlet total temperature for Jet A and liquefied natural gas at ambient temperature. Combustor inlet total pressure, P_3, 6 atmospheres; reference Mach number, 0.065.

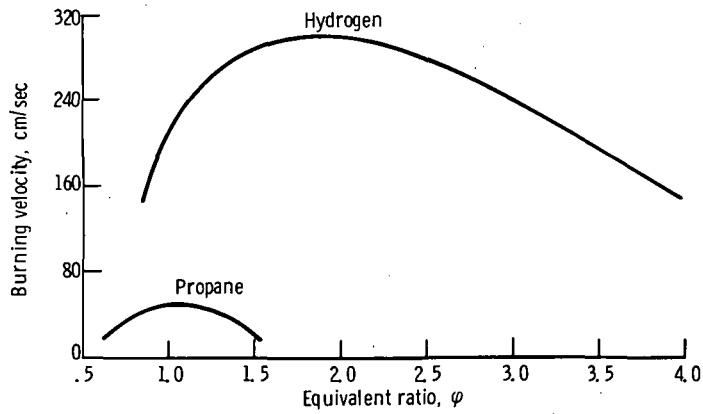

Figure 34. - Burning velocities for hydrogen and propane.

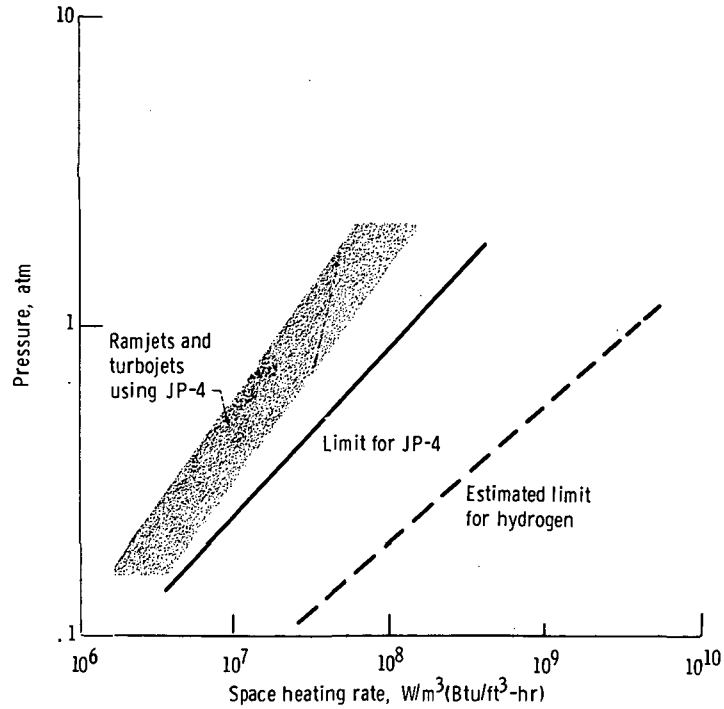

Figure 35. - Space heating rates for JP-4 and hydrogen.

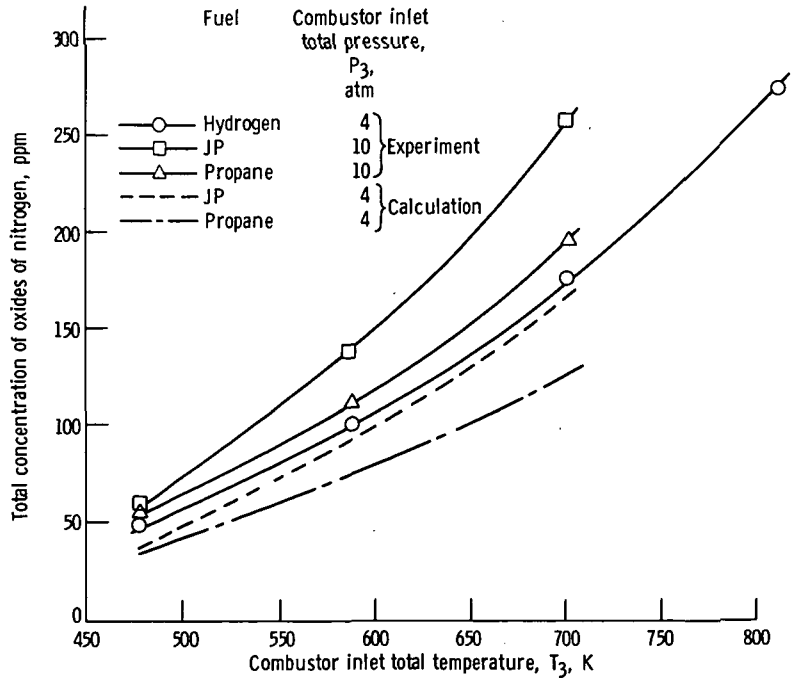

Figure 36. - Effect of combustor inlet total temperature on oxides-of-nitrogen emissions from an experimental combustor. Combustor temperature differential, 650 K.

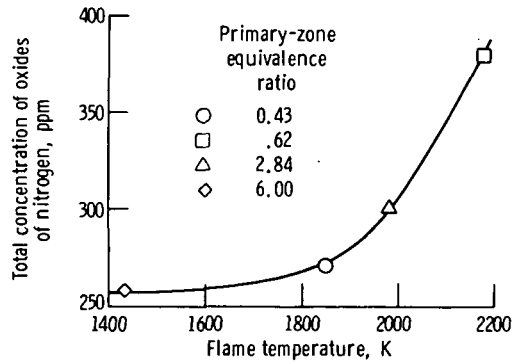

Figure 37. - Effect of flame temperature on oxides-of-nitrogen emissions from an experimental combustor using hydrogen fuel. Combustor inlet total temperature, T_3, 810 K; temperature differential, 650 K; combustor inlet total pressure, P_3, 4 atmospheres; overall equivalence ratio, φ, 0.22.

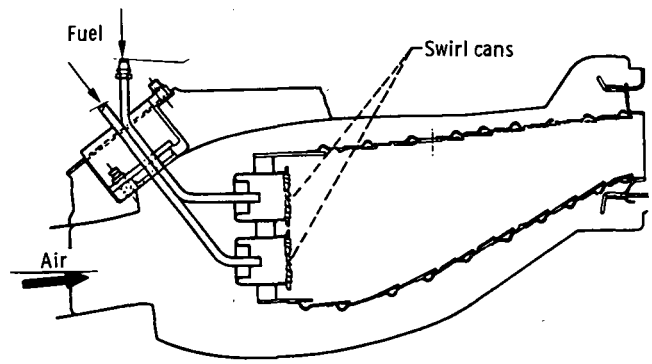

Figure 38. - NASA swirl-can modular combustor for CF6-50 engine.

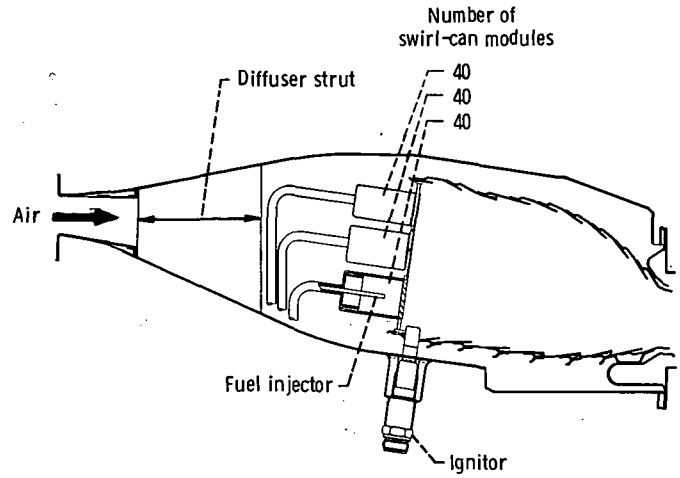

Figure 39. - NASA swirl-can modular combustor for JT9D engine.

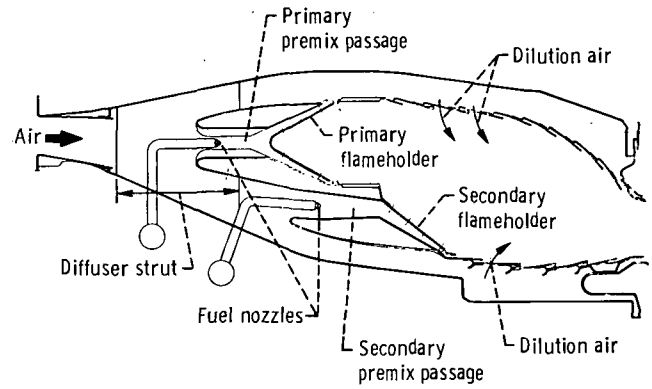

Figure 40. - Staged premix combustor for JT9D engine.

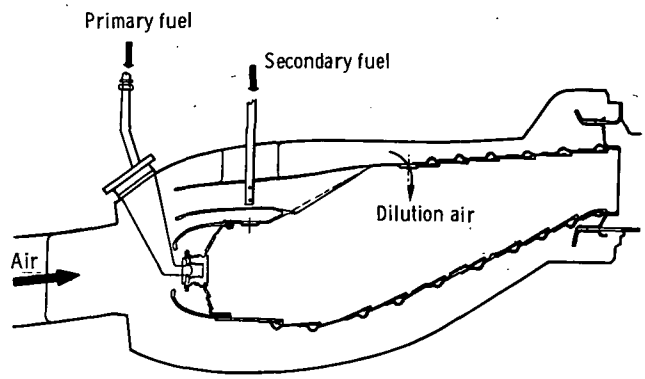

Figure 41. - Radial/axial staged combustor for CF6-50 engine.

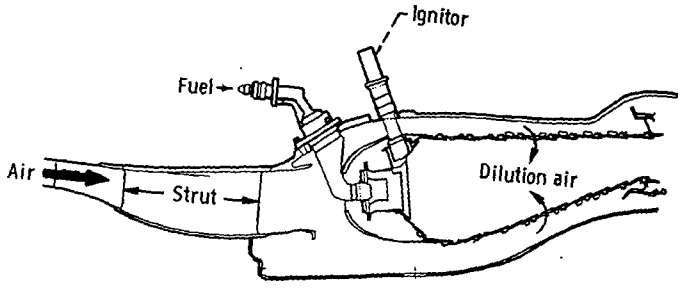

Figure 42. - Single-annular, lean-dome combustor for CF6-50 engine.

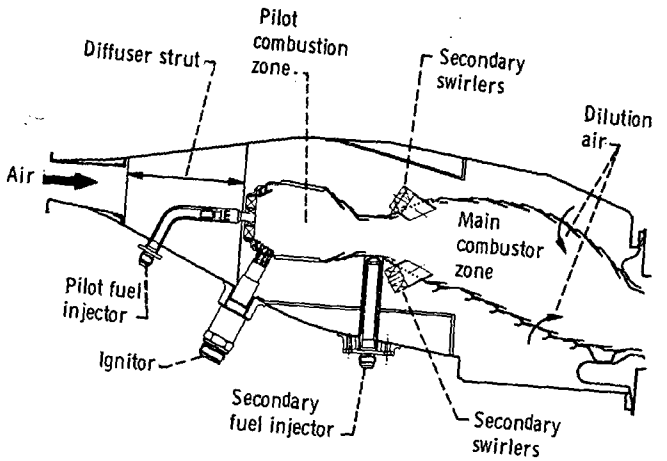

Figure 43. - Swirl combustor for JT9D engine.

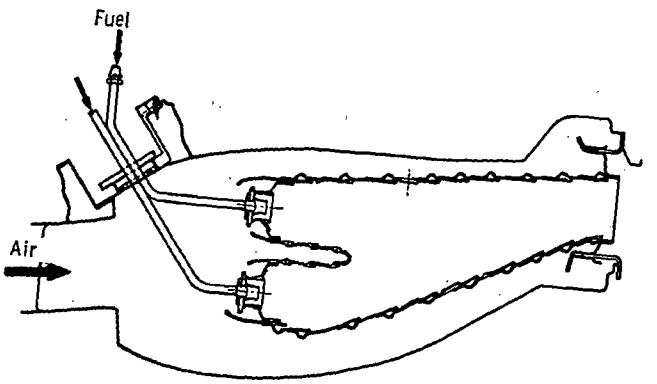

Figure 44. - Double-annular, lean-dome combustor for CF6-50 engine.

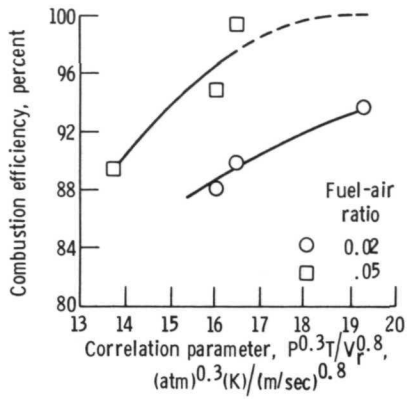

Figure 45. - Influence of combustor inlet pressure-temperature-velocity correlation parameter on combustion efficiency of an experimental duct burner.

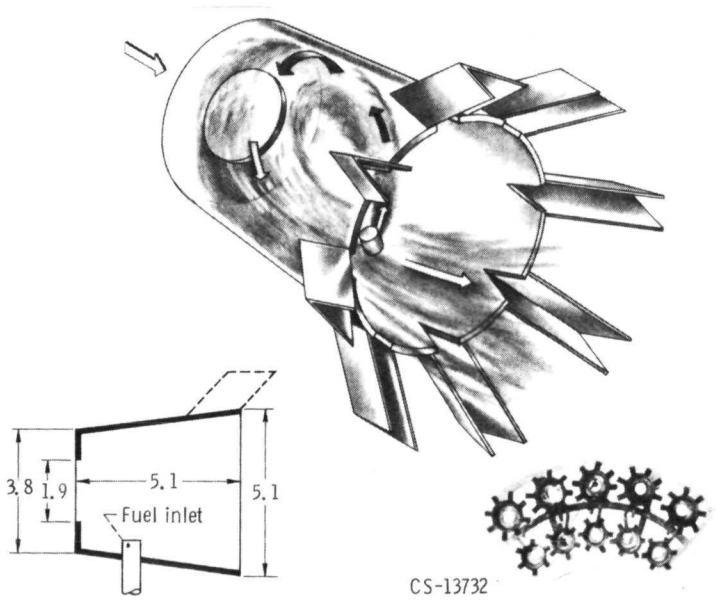

Figure 46. - Hydrogen-fueled quarter-sector test combustor and swirl-can element. (Dimensions are in centimeters.)

Figure 47. - Swirl-can combustor for hydrogen-fueled turbojet engine, view looking upstream.

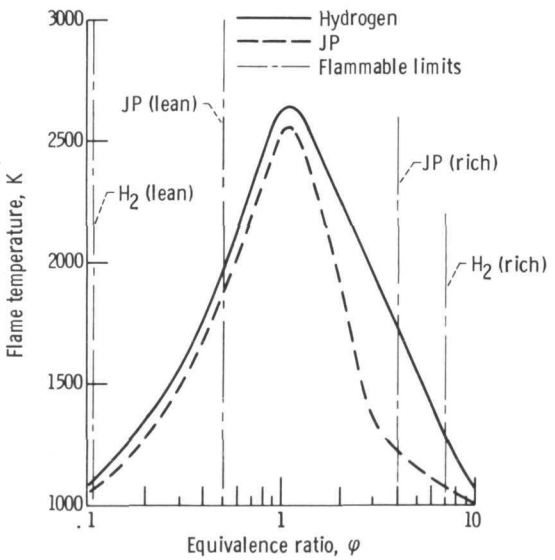

Figure 48. - Theoretical flame temperature. Combustor inlet total temperature, T_3, 800 K; combustor inlet total pressure, P_3, 5 atmospheres.

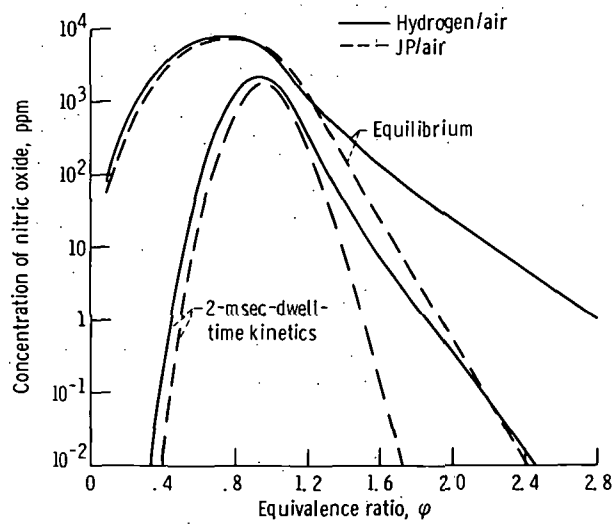

Figure 49. - Theoretical nitric oxide concentrations. Combustor inlet total temperature, T_3, 800 K; combustor inlet total pressure, P_3, 5 atmospheres.

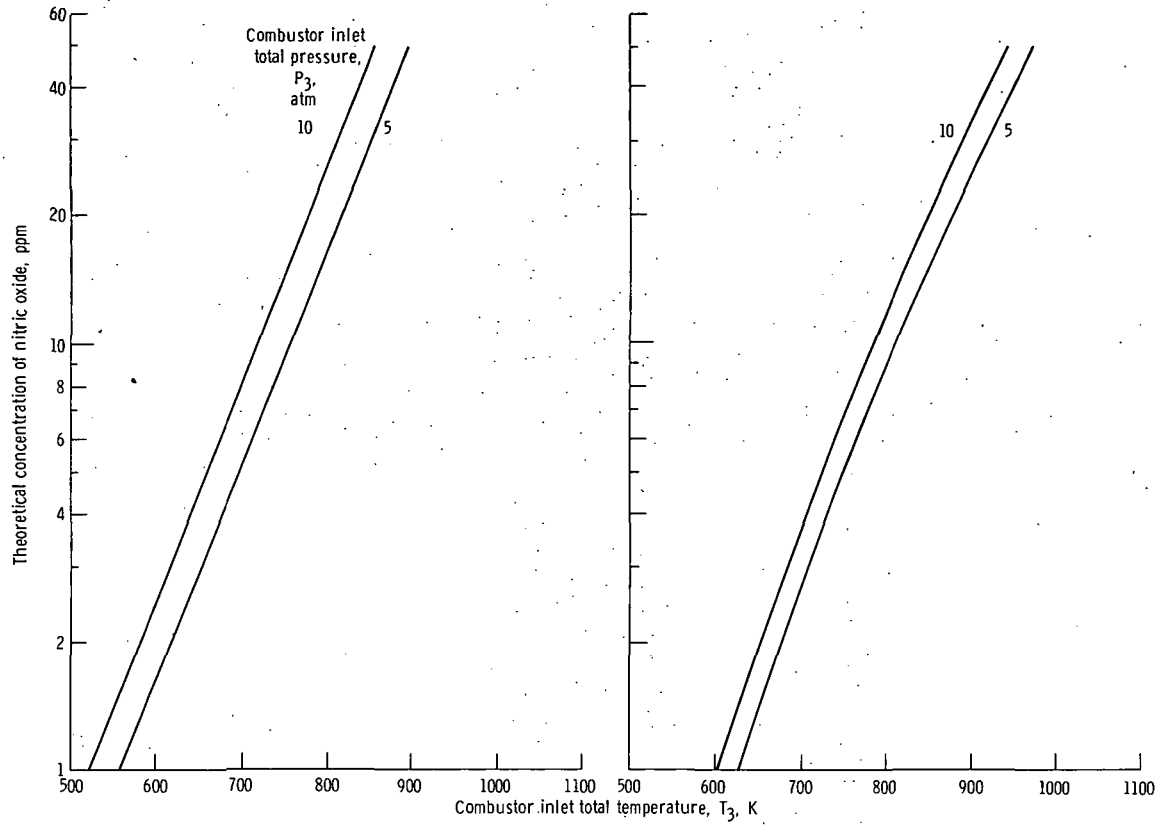

(a) JP fuel; primary-zone equivalence ratio, φ, 0.6.

(b) LNG fuel; primary-zone equivalence ratio, φ, 0.6.

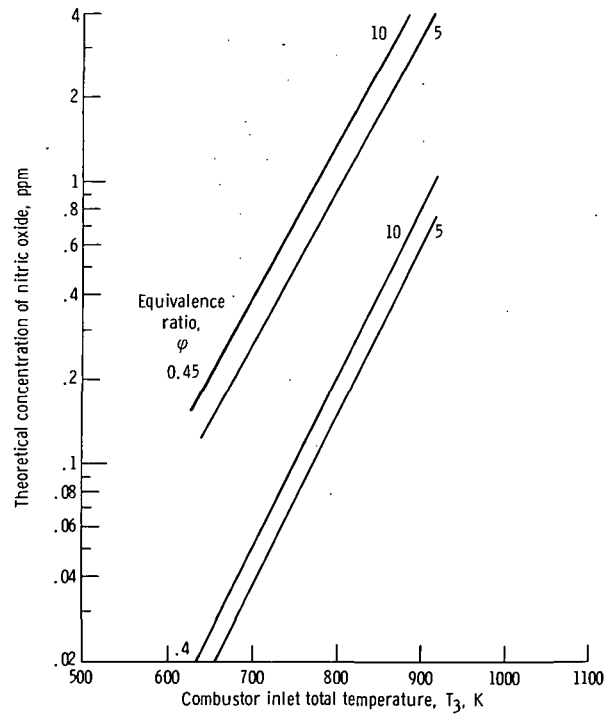

(c) Hydrogen fuel.

Figure 50. - Variation of theoretical nitric oxide concentration with combustor inlet total temperature. Primary-zone dwell time, 2 milliseconds.

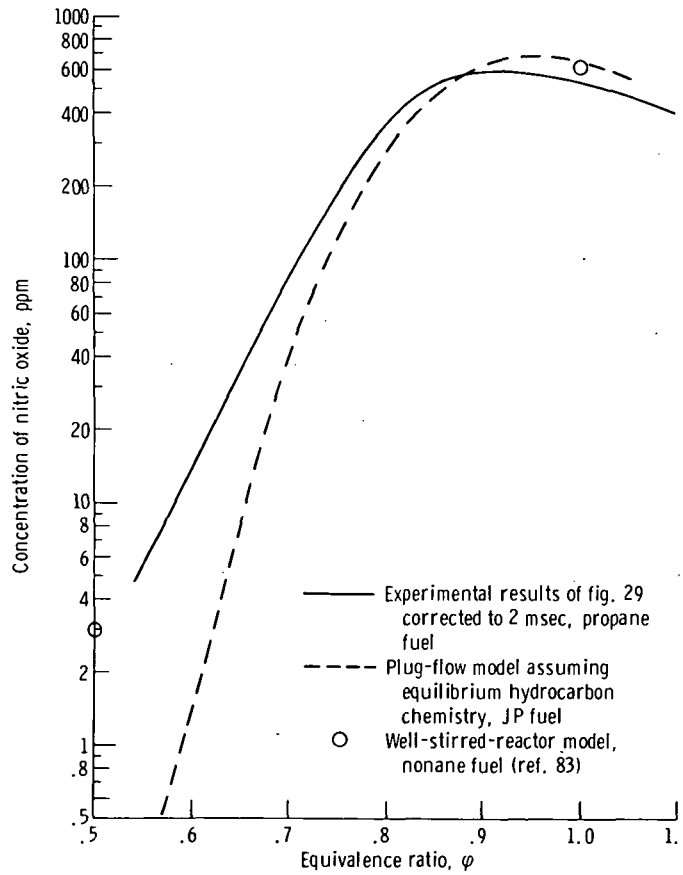

Figure 51. - Comparison between experimental and theoretical nitric oxide concentrations for a premixed, prevaporized reactor. Combustor inlet total temperature, T_3, 590 K; combustor inlet total pressure, P_3, 5 atmospheres; dwell time, 2 milliseconds.

NASA-Langley, 1974 E-7822

NATIONAL AERONAUTICS AND SPACE ADMINISTRATION
WASHINGTON, D.C. 20546

OFFICIAL BUSINESS
PENALTY FOR PRIVATE USE $300

SPECIAL FOURTH-CLASS RATE
BOOK

POSTAGE AND FEES PAID
NATIONAL AERONAUTICS AND
SPACE ADMINISTRATION
451

U.S.MAIL

POSTMASTER: If Undeliverable (Section 158 Postal Manual) Do Not Return

"The aeronautical and space activities of the United States shall be conducted so as to contribute . . . to the expansion of human knowledge of phenomena in the atmosphere and space. The Administration shall provide for the widest practicable and appropriate dissemination of information concerning its activities and the results thereof."

—NATIONAL AERONAUTICS AND SPACE ACT OF 1958

NASA SCIENTIFIC AND TECHNICAL PUBLICATIONS

TECHNICAL REPORTS: Scientific and technical information considered important, complete, and a lasting contribution to existing knowledge.

TECHNICAL NOTES: Information less broad in scope but nevertheless of importance as a contribution to existing knowledge.

TECHNICAL MEMORANDUMS: Information receiving limited distribution because of preliminary data, security classification, or other reasons. Also includes conference proceedings with either limited or unlimited distribution.

CONTRACTOR REPORTS: Scientific and technical information generated under a NASA contract or grant and considered an important contribution to existing knowledge.

TECHNICAL TRANSLATIONS: Information published in a foreign language considered to merit NASA distribution in English.

SPECIAL PUBLICATIONS: Information derived from or of value to NASA activities. Publications include final reports of major projects, monographs, data compilations, handbooks, sourcebooks, and special bibliographies.

TECHNOLOGY UTILIZATION PUBLICATIONS: Information on technology used by NASA that may be of particular interest in commercial and other non-aerospace applications. Publications include Tech Briefs, Technology Utilization Reports and Technology Surveys.

Details on the availability of these publications may be obtained from:

SCIENTIFIC AND TECHNICAL INFORMATION OFFICE

NATIONAL AERONAUTICS AND SPACE ADMINISTRATION

Washington, D.C. 20546